2006

A rapid method for approximating invariant manifolds of differential equations

Tang, Shouchun (Terry)

Lethbridge, Alta. : University of Lethbridge, Faculty of Arts and Science, 2006

A RAPID METHOD FOR APPROXIMATING INVARIANT MANIFOLDS OF DIFFERENTIAL EQUATIONS

SHOUCHUN (TERRY) TANG

B.Sc. in Biochemistry, University of Alberta, 2003

A thesis

Submitted to the School of Graduate Studies

of the University of Lethbridge

in Partial Fulfilment of the

Requirements for the Degree

MASTER OF SCIENCE IN BIOCHEMISTRY

Department of Chemistry and Biochemistry

University of Lethbridge

LETHBRIDGE, ALBERTA, CANADA

ABSTRACT

The Intrinsic Low-Dimensional Manifold (ILDM) has been adopted as an approximation to the slow manifold representing the long-term evolution of a non-linear chemical system. The computation of the slow manifold simplifies the model without sacrificing accuracy because the trajectories are rapidly attracted to it. The ILDM has been shown to be a highly accurate approximation to the manifold when the curvature of the manifold is not too large. An efficient method of calculating an approximation to the slow manifold which may be equivalent to the ILDM is presented. This method, called Functional Equation Truncation (FET), is based on the assumption that the local curvature of the manifold is negligible, resulting in a locally linearized system. This system takes the form of a set of algebraic equations which can be solved for given values of the independent variables. Two-dimensional and three-dimensional models are used to test this method. The approximations to one-dimensional slow manifolds computed by FET are quite close to the corresponding ILDMs and those for two-dimensional ones seem to differ from their ILDM counterparts.

ACKNOWLEDGEMENTS

With gratitude, I acknowledge the excellent supervision of Professor Marc R. Roussel whose knowledge, encouragement, and patience were instrumental in constructing this thesis. I also thank the Department of Chemistry and Biochemistry and all the fellow graduate students for the learning environment they provide.

Contents

List of Figures

Chapter 1

Introduction

Chemical and biochemical reactions typically involve many species including reactants, intermediates, and products, and take place on time scales stretching from femtoseconds to years. People who study these reactions analytically are fond of the freedom of knowing the concentration correlations among the species throughout the course of the reaction. Because of the transitoriness of most intermediates, among many other factors, modern measuring devices are often unable to capture the instantaneous concentration of all the species at the same time. Therefore, people are impelled to use mathematical models to express the interrelations among species to help monitor and control system behaviour. These chemical models often take the form of non-linear differential equations that generally do not have analytical solutions. The obvious solution to this problem is to compute them numerically, which is done by assuming an initial condition for each concentration variable and using a very small time interval δt to replace the infinitesimal dt to calculate the concentrations at the next time point. This approach can be quite easily carried out on modern computers, but it has limitations. One of the major limitations is that the number of differential equations generated can be very high even for only a few coupled reaction pathways making the

computational time required correspondingly long. The other is that the interpretation of simulation results is difficult because of the lack of understanding of the correlation between species.

An alternative way to solve the problems associated with chemical modelling is to reduce the model and to find analytical approximations to the real solution(s). Over the last decade or so, various model reduction methods have been developed [2, 6–10, 15–17, 22, 24, 26, 29]. Most of these methods take advantage of the fact that chemical species often relax in hierarchical order [3, 11, 28]. From a geometrical point of view, the chemical species in the mathematical model are attracted to surfaces of increasingly lower dimension that are collectively called *slow invariant manifolds* or simply *slow manifolds* [7]. The purpose of this thesis is to introduce a new model reduction method that approximates various levels of slow manifold with reasonable accuracy and speed.

To start, let us examine some simple methods that separate hierarchical relaxation order.

1.1 Steady-state approximation

Below is a simple enzyme-kinetics mechanism first proposed by Wurtz [31] in 1880 and popularised by Leonor Michaelis and Maud Menten [20] (after whom it is named) in the early 20th century:

$$E + S \underset{k_{-1}}{\overset{k_1}{\rightleftharpoons}} C \xrightarrow{k_2} E + P,$$

where E is the enzyme, S is the substrate, P is the product, and C is called the Michaelis complex, which is the intermediate between the substrate and the product, generated by combining one molecule of the substrate and one molecule of the enzyme. The k's are the rate constants.

This reaction mechanism can be mathematically represented with the following system of equations:

$$\dot{E} = -k_1 ES + k_2 C + k_{-1} C, \tag{1.1a}$$

$$\dot{S} = -k_1 ES + k_{-1} C, \tag{1.1b}$$

$$\dot{C} = k_1 ES - k_2 C - k_{-1} C, \tag{1.1c}$$

$$\dot{P} = k_2 C \tag{1.1d}$$

where the capital letters represent the concentrations of the corresponding chemical species and the dots above them are used to denote time derivatives so that, for example, $\dot{E} = \frac{dE}{dt}$.

Other than the equations above, there are some values in the reaction that are conserved throughout. For every reacted molecule of S, one molecule of C is generated and when this molecule of C reacts further, one molecule of P is produced. Therefore,

$$S + C + P = S_0. \tag{1.2}$$

S_0 is a constant that depends on the initial concentrations in a particular experiment. Similarly, there is another obvious conservation equation:

$$E + C = E_0, \tag{1.3}$$

where, again, E_0 is constant.

The significance of equations (1.2) and (1.3) is that they allow any two species concentrations to be calculated from the other two. As a consequence, the original rate equations can be reduced so that fewer variables still carry the same amount of information.

The reduced system from equations (1.1) is

$$\dot{S} = -k_1 (E_0 - C) S + k_{-1} C, \tag{1.4a}$$

$$\dot{C} = k_1(E_0 - C)S - k_2C - k_{-1}C. \tag{1.4b}$$

Although we have now reduced the system from four differential equations to only two, they still cannot be solved analytically. Further reduction is required.

One of the analytical methods, the *equilibrium approximation* or EA, exploits the assumption of equilibrium for the first step and is valid if the second step of the reaction is much slower than the backward reaction of the first step, i.e., if $k_{-1} \gg k_2$:

$$\frac{ES}{C} = \frac{k_{-1}}{k_1} = \frac{(E_0 - C)S}{C}. \tag{1.5}$$

Using this equation to replace $(E_0 - C)S$ in equation (1.4b), one can integrate equation (1.4b) to yield

$$C = Me^{-k_2 t},$$

where M is an integration constant. By substituting the result for C back into equation (1.5), S can be obtained as:

$$S = \frac{k_{-1}Me^{-k_2 t}}{k_1(E_0 - Me^{-k_2 t})}.$$

Another method makes the assumption that the substrate concentration is in great excess over the enzyme concentration ($S \gg E$) which is often true under *in vitro* conditions. With the exception of the initial stage of the reaction, which is usually very brief compared to the whole course, C remains approximately constant until the substrate is nearly exhausted. Therefore, the rate of consumption of C is the same as the rate of synthesis, which means C is at a steady state, and the assumption is called the *steady state assumption*, or SSA [1]. This assumption implies the following equation:

$$\frac{dC}{dt} = 0.$$

Substitute the above into equation (1.4b) so that C can be solved for as a function of S:

$$C = \frac{k_1 E_0 S}{k_1 S + k_2 + k_{-1}}.$$

By substituting it into equation (1.4a), one can obtain the degenerated differential equation:

$$\dot{S} = -\frac{k_1 k_2 E_0 S}{S k_1 + k_2 + k_{-1}}. \tag{1.6}$$

The integrated form of this result, implicitly, is

$$(k_{-1} + k_2) \ln S + S k_1 = -k_1 k_2 E_0 t.$$

This solution tends to the solution of equations (1.4) as long as the condition for the SSA holds.

1.2 Fraser's iterative method

Ever since the equilibrium and steady-state approximations were proposed, a fair amount of attention has been devoted to these two methods. Most of this work was directed toward either finding the conditions under which these two methods are valid or generalizing them so that they can be applied to mechanisms that have more steps. Despite all the studies on SSA and EA, they still have some unresolvable disadvantages. Among the most important is that the approximations they make do not belong to a hierarchy that allows the true solution to be asymptotically approached, making further work based on them not very promising.

In order to further approach the true solution, another method is proposed by Fraser [7]. For autonomous Ordinary Differential Equations (ODEs), i.e. equations in which the rates of change do not depend explicitly on time, the time variable can be eliminated altogether by parameterizing the species variables with respect to one another and by applying the chain rule:

$$C = C(S),$$

thus

$$\frac{dC}{dt} = \frac{dC}{dS}\frac{dS}{dt};$$

so that, using equations (1.4),

$$\frac{dC}{dS} = \frac{dC/dt}{dS/dt} = \frac{k_1(E_0 - C)S - k_2C - k_{-1}C}{-k_1(E_0 - C)S + k_{-1}C}. \tag{1.7}$$

As there is no assumption or truncation made to the ODEs in obtaining equation (1.7), its solution represents the exact relation between S and C. Unfortunately, equation (1.7) for most systems does not have an analytical solution, but an iterative method can be used to find the solution(s).

Assume an initial guess for C as a function of S:

$$C = C_0(S).$$

Then differentiate this function with respect to S so that dC/dS is a function of S (denoting dC/dS by C'):

$$C' = C_0'(S).$$

Substitute the above into the left-hand side of equation (1.7) and solve for C, again as a function of S. The procedures of differentiation and substitution can be repeated to eventually reach the true solution, provided that the iterations converge [25].

1.3 Singular Perturbation Approaches

Fraser's functional iteration method is a good way to solve a non-linear autonomous dynamical system for the slow manifolds. Through enough steps of iteration, the iterates can asymptotically approach the true result. The drawback with this method, however, is that it requires that the system is well behaved which means the iteration steps must carry the

solutions for each step closer and closer to the true one. In reality, not all systems can be assumed to behave that way, especially when the initial guess is arbitrary. The chance for these solutions to converge can be significantly improved by having a good initial starting function. This makes it important for the initial guess to be obtained by other means.

Let us now examine the SSA more closely. If the amount of substrate is large compared to the amount of enzyme, the Michaelis-Menten reaction can be partitioned into three separate phases:

1. While S is large, E is small, and C is 0, the first step of the reaction takes place very quickly and C increases very fast until the system enters the second phase.

2. The system reaches a steady state where C and E remain virtually constant and S decreases slowly. This state remains for most of the overall reaction time.

3. After S has decreased sufficiently to be comparable to E_0 (the initial value of E), the steady state condition no longer holds. The substrate concentration is no longer enough to tie up the enzyme and C starts to decrease. In the end, all the substrate is turned into the product.

Through this analysis, one can see that the chemical species involved in a reaction relax in hierarchical order. By finding and separating the hierarchical order, one can discard the fast responses while retaining the slow-evolving ones, which are more significant and can be observed through experiments. One such method is called *Singular Perturbation.* This method can not only be related to the steady-state approximation but also provide an explicit mathematical justification for the assumption of steady state [12].

The Michaelis-Menten mechanism can be used again to illustrate the singular perturbation method. First, some new variables are defined. Notice that all the new variables are

dimensionless, which means they do not have any units:

$$s = \frac{S}{S_0}, \qquad c = \frac{C}{E_0}, \qquad \mu = \frac{E_0}{S_0},$$

$$\tau = k_1 E_0 t, \qquad \alpha = \frac{(k_{-1}+k_2)}{k_1 S_0}, \qquad \beta = \frac{k_2}{k_1 S_0},$$

where S_0 is the initial concentration of S. Throughout this work, lower-case letters are used to denote species variables that are dimensionless.

With this transformation, equations (1.4) become

$$\dot{s} = -s + (s + \alpha - \beta)c, \tag{1.8a}$$

$$\mu\dot{c} = s - (s + \alpha)c. \tag{1.8b}$$

If $\mu \equiv \frac{E_0}{S_0} \to 0$, the left-hand side of equation (1.8b) becomes 0 as well, reducing equation (1.8b) to an algebraic equation. With this algebraic equation, c can be explicitly expressed as a function of s which can be substituted into equation (1.8a) to give

$$\dot{s} = -\frac{\alpha s}{s + \alpha}. \tag{1.9}$$

The solution of equation (1.9) is an approximation to motion on the slow manifold of the ODEs as $\mu \to 0$. This assertion is made because E_0/S_0 is very small, which means, biochemically speaking, that the enzyme concentration is minute compared to that of the substrate. This is the same assumption made before. This is in fact a rationale for the steady-state assumption, and equation (1.9) is the dimensionless form of equation (1.6).

1.4 Hidden Hierarchical Order

While the singular perturbation approach is a good way to separate the relaxation time scales, some systems have hierarchical relaxation that is hidden and cannot be extracted by transformation of variables. Therefore, methods that can exploit the hidden order are in demand.

The next chapter reviews one of the best-known methods (developed by Maas and Pope [19]) to make visible the hidden order and approximate the slow manifold. As the results obtained by their method can be compared with the ones produced by our method, it is necessary to describe it in detail.

Chapter 2

Background Knowledge

2.1 Differences between linear and non-linear systems

2.1.1 Solution of linear ODEs

To understand the reason why non-linear ODEs cannot be analytically solved, The method used to solve linear ODEs must first be reviewed.

Consider the autonomous system of differential equations that represents a well-mixed chemical or biochemical system (bold letters are used to denote vectors):

$$\dot{\mathbf{x}} = \mathbf{f}(\mathbf{x}), \tag{2.1}$$

where $\mathbf{x}$ is a vector of state variables (e.g., concentrations, temperature) and $\dot{\mathbf{x}}$ is the time derivative. The solution of equation (2.1) is in the form of $\mathbf{x}$ as a function of t. To find the solution, expand the right hand side (RHS) of the equation about its equilibrium point $\mathbf{x}^*$ (the point where $\dot{\mathbf{x}} = \mathbf{f}(\mathbf{x}^*) = 0$) using a Taylor series. The result is

$$\begin{aligned}
\dot{\mathbf{x}} &= \mathbf{f}(\mathbf{x}^*) + \left.\frac{\partial \mathbf{f}}{\partial \mathbf{x}}\right|_{\mathbf{x}^*} (\mathbf{x} - \mathbf{x}^*) + (\mathbf{x} - \mathbf{x}^*)^{\mathbf{T}} \left.\frac{\partial^2 \mathbf{f}}{\partial \mathbf{x}^2}\right|_{\mathbf{x}^*} (\mathbf{x} - \mathbf{x}^*) + \dots \\
&= \left.\frac{\partial \mathbf{f}}{\partial \mathbf{x}}\right|_{\mathbf{x}^*} (\mathbf{x} - \mathbf{x}^*) + (\mathbf{x} - \mathbf{x}^*)^{\mathbf{T}} \left.\frac{\partial^2 \mathbf{f}}{\partial \mathbf{x}^2}\right|_{\mathbf{x}^*} (\mathbf{x} - \mathbf{x}^*) + \dots
\end{aligned}$$

where the superscript in $(\mathbf{x} - \mathbf{x}^*)^{\mathrm{T}}$ represents the matrix transpose and $\left.\frac{\partial^2 \mathbf{f}}{\partial \mathbf{x}^2}\right|_{\mathbf{x}^*}$ is the Hessian tensor. For a linear system, everything in $\mathbf{f}(\mathbf{x})$ is first-order so that

$$\left.\frac{\partial^2 \mathbf{f}}{\partial \mathbf{x}^2}\right|_{\mathbf{x}^*} = 0.$$

The same assumption is made for all the higher order derivatives. The differential equation can be exactly written as

$$\dot{\mathbf{x}} = \left.\frac{\partial \mathbf{f}}{\partial \mathbf{x}}\right|_{\mathbf{x}^*} (\mathbf{x} - \mathbf{x}^*). \tag{2.2}$$

The partial derivative in the equation above is called the *Jacobian matrix*. Suppose the components in the vector $\mathbf{x}$ are $(x_1, x_2, \cdots, x_n)$ and the components in the vector $\mathbf{f}$ are $(f_1, f_2, \cdots, f_n)$; then the Jacobian is defined as:

$$\mathbf{J} = \begin{bmatrix} \frac{\partial f_1}{\partial x_1} & \frac{\partial f_1}{\partial x_2} & \cdots & \frac{\partial f_1}{\partial x_n} \\ \frac{\partial f_2}{\partial x_1} & \frac{\partial f_2}{\partial x_2} & \cdots & \frac{\partial f_2}{\partial x_n} \\ \vdots & \vdots & \ddots & \vdots \\ \frac{\partial f_n}{\partial x_1} & \frac{\partial f_n}{\partial x_2} & \cdots & \frac{\partial f_n}{\partial x_n} \end{bmatrix}.$$

If we define $\mathbf{y} = \mathbf{x} - \mathbf{x}^*$, equation (2.2) can be rewritten as

$$\dot{\mathbf{y}} = \mathbf{J}\mathbf{y}. \tag{2.3}$$

The solution is

$$y(t) = c_1 e^{\lambda_1 t}\mathbf{v_1} + c_2 e^{\lambda_2 t}\mathbf{v_2} + \cdots + c_n e^{\lambda_n t}\mathbf{v_n}, \tag{2.4}$$

where the λ_i's are unique eigenvalues of $\mathbf{J}$ and the $\mathbf{v_i}$'s are their corresponding eigenvectors. The constants denoted by c_i depend on the starting point of the system. The proof of this solution can be found in most differential equations textbooks [30].

2.1.2 Non-linear ODEs

Similar ideas involving Jacobians and eigen-analysis can be used to deal with non-linear systems with some additional considerations. With linear differential equations, because everything is first order, the partial differentiations leave the Jacobian constant. This is not the case for a non-linear system because there are second- or higher-order terms that leave variables in the Jacobian. However, we can evaluate the Jacobian at a point in phase space by substituting the coordinates of that point into the Jacobian to compute its eigenvalues and eigenvectors there.

Let $\mathbf{x_1}$ and $\mathbf{x_2}$ be two nearby but otherwise arbitrary points in phase space. Define

$$\delta\mathbf{x} = \mathbf{x_2} - \mathbf{x_1}.$$

The time derivative of $\delta\mathbf{x}$, therefore, is

$$\delta\dot{\mathbf{x}} = \dot{\mathbf{x_2}} - \dot{\mathbf{x_1}} = \mathbf{f}(\mathbf{x_2}) - \mathbf{f}(\mathbf{x_1}) = \mathbf{f}(\mathbf{x_1} + \delta\mathbf{x}) - \mathbf{f}(\mathbf{x_1}).$$

The Taylor expansion of $\mathbf{f}(\mathbf{x_1} + \delta\mathbf{x})$ about the point $\mathbf{x_1}$ is

$$\mathbf{f}(\mathbf{x_1} + \delta\mathbf{x}) = \mathbf{f}(\mathbf{x_1}) + \mathbf{J_1}\delta\mathbf{x} + \ldots$$

where $\mathbf{J_1}$ is the Jacobian evaluated at $\mathbf{x_1}$. Substitution of this expansion into $\delta\dot{\mathbf{x}} = \mathbf{f}(\mathbf{x_1} + \delta\mathbf{x}) - \mathbf{f}(\mathbf{x_1})$ with the higher-order terms truncated yields

$$\delta\dot{\mathbf{x}} \approx \mathbf{J_1}\delta\mathbf{x}. \tag{2.5}$$

Using a similar eigenvalue and eigenvector analysis to equation (2.3), equation (2.5) can be used to gain insight into the *local* trend of evolution of the trajectories around $\mathbf{x_1}$. Globally, each distinctive point has its unique Jacobian matrix, and the eigen-analysis is only valid locally.

2.2 Classical ILDM method

2.2.1 Questions leading to ILDM

With most chemical systems, there typically are fast and slow reaction processes that take place on different time scales and divide the course of the overall reaction. The fast processes relax faster than the slower ones. However, fast processes do not necessarily coincide with fast elementary reactions. Some reaction steps may have a large rate coefficient, but if these steps require as their reactants the products of steps with smaller rate coefficients, their actual reaction rates can be no faster than those of the preceding steps. Therefore, processes that take place during later time intervals must be equally fast or slower than the ones that take place during earlier ones, making the overall reaction slower and slower. As far as chemical species are concerned, we say that they relax in hierarchical order. Singular perturbation as discussed in the previous section is an example of a method that exploits this separation of time scales.

The major limitation of singular perturbation is that not all systems can be transformed into the singular perturbation form, with a small parameter multiplying a time derivative. Even for the ones that can be, it may be very difficult. For these systems, the hierarchical order is considered *hidden*. A better method is needed to exploit the hidden hierarchical order. The classical ILDM (Intrinsic Low-Dimensional Manifold) method proposed by Maas and Pope is designed to achieve this.

Based on the discussion in section (2.1), any autonomous ODE (linear or non-linear) can be Taylor expanded to a form which is generally shown as

$$\delta\dot{\mathbf{x}} = \left.\frac{\partial \mathbf{f}}{\partial \mathbf{x}}\right|_{\mathbf{x}^*} (\mathbf{x}-\mathbf{x}^*) + (\mathbf{x}-\mathbf{x}^*)^{\mathbf{T}} \left.\frac{\partial^2 \mathbf{f}}{\partial \mathbf{x}^2}\right|_{\mathbf{x}^*} (\mathbf{x}-\mathbf{x}^*) + \cdots$$

With the less significant higher order derivatives being assumed to be 0 and the Jacobian

being denoted by $\mathbf{J}$, the simplified ODE is

$$\delta\dot{\mathbf{x}} = \mathbf{J}\delta\mathbf{x}.$$

The hierarchical order is hidden in the matrix $\mathbf{J}$ and we want to obtain the slower-reacting processes.

Equation (2.4) is the solution for linear ODEs. It dictates the dynamics of the concentration variables by decomposing the motion into its components along each eigenvector. The $c_i e^{\lambda_i t}$ term multiplying each eigenvector, on the other hand, controls how strongly this eigenvector influences the overall motion; a higher magnitude means the overall motion is more parallel to the corresponding eigenvector and *vice versa*. For a closed chemical or biochemical system that converges at every local position, the λ_i's must all be negative to assure $\delta\mathbf{x}$ decrease as t increases. While t increases, the magnitude of the $e^{\lambda_i t}$ terms decrease, especially for those that have more negative λ_i's. For these more rapidly decreasing terms, their influence on the trajectory diminishes as well, and eventually only the terms that have less negative λ_i's influence the trajectory. Since for linear systems, trajectories from all over the phase space share the same eigenvalues and eigenvectors, they tend to be attracted to the same eigenspace spanned by the eigenvectors associated with the less negative eigenvalues (call these eigenvectors *slow eigenvectors*). The surface (or hyper-surface) is called the *invariant manifold.*

Things are similar for a non-linear ODE except that the Jacobian matrix still contains concentration variables. The consequence is that it's difficult to compare the magnitudes of the eigenvalues because they have different values at different places in phase space. To tackle this problem, real values can be assigned to the concentration variables so that the Jacobian is similar to that for a linear system. As a drawback, the eigen-analysis is valid only in the vicinity of the point defined by the values of the variables. In other words, the analysis

is *local* as opposed to *global*, the latter being the case for linear systems. In the global picture for a nonlinear system, every point in the phase space has its unique Jacobian, hence unique sets of eigenvalues and eigenvectors. However, other than some special cases, the magnitudes of eigenvalues and the directions of eigenspaces among points that are close to one another are similar and depend continuously on the variables. Based on this observation, we can first analyze the equilibrium point where the influence of each eigenvector is zero and find the slowest eigenvector (the vector whose corresponding eigenvalue is the least negative). Then we follow this eigenvector backward in time and this will sketch out a trajectory on which each point, if allowed to run forward in time, can reach the equilibrium along it. As long as there are no drastic changes along the path of this trajectory (call it the "*slow trajectory*") such as eigenvalues changing order or real eigenvalues becoming complex, the chosen slowest eigenvector is the slowest throughout the path. If a stable equilibrium point can be thought of as a point whose movement is the slowest (no movement at all), then the slow trajectory is a collection of points, each of which moves faster than the equilibrium but slower than all other points in its vicinity, excluding ones from the same collection. For a contracting system, because the influences of the faster eigenvectors diminish, the slowest eigenvector dictates the flow of a trajectory. Therefore, all trajectories are attracted to the slow trajectory.

Imagine a phase space that has n dimensions. The number of eigenvectors is n. If they are all non-degenerate, they can be ranked from the slowest to the fastest according to their corresponding eigenvalues. The fastest eigenvector is the first one to lose influence; the second fastest is the second; and so on. As a consequence, a trajectory, starting in an n-dimensional space, is first attracted to an $(n-1)$-dimensional space spanned by the slowest $n-1$ eigenvectors. Within this $(n-1)$-dimensional space, there is an $(n-2)$-

dimensional space spanned by the slowest $n-2$ eigenvectors. The process of attracting goes on and the slow trajectory, which is a one-dimensional space spanned by the single slowest eigenvector, serves as the last space that attracts trajectories before they reach equilibrium. These attracting spaces (surfaces) of various dimension are called *slow invariant manifolds*, or simply *slow manifolds*.

The classical ILDM is a method that is designed to find the slow manifolds of a system. To understand this method, two algebraic operations that are performed on the Jacobian need to be introduced.

2.2.2 Schur Decomposition

The Schur decomposition is a procedure that can be applied to a square matrix so that the matrix can be decomposed as the product of three matrices:

$$\mathbf{A} = \mathbf{Q^H N Q}.$$

The three matrices have some special properties: Q is a unitary matrix ($\mathbf{Q^H} = \mathbf{Q^{-1}}$ where $\mathbf{Q^H}$ denotes the conjugate transpose of $\mathbf{Q}$: $\mathbf{Q^H} \equiv \overline{\mathbf{Q^T}}$). $\mathbf{N}$ is an upper triangular matrix with the diagonal entries being the eigenvalues of $\mathbf{A}$. The columns of $\mathbf{Q}$ define the eigenspace of the original matrix $\mathbf{A}$ with the first column denoting the unit eigenvector associated to the eigenvalue on the first entry of $\mathbf{N}$ and the rest of the columns are adjusted so that they are orthonormal to each other. The columns other than the first one are not necessarily the eigenvectors. In fact, they are unlikely to be the eigenvectors. Moreover, the first k column vectors in $\mathbf{Q}$ form a basis for the subspace spanned by the eigenvectors associated with the first k eigenvalues listed in $\mathbf{N}$.

2.2.3 Givens Rotation

A Givens rotation rearranges the result of Schur decomposition so that *the smallest eigenvalue ends up being the last entry in* $\mathbf{N}$ *and the largest one being the first entry.* All the others on the diagonal of $\mathbf{N}$ are in descending order. Suppose there are n columns in $\mathbf{Q}$; the first k columns span the fast-decaying or short-lasting eigenspace.

2.2.4 Core ideas of ILDM

Because a slow manifold of a system determines the long-term trend of the trajectories, the idea of the ILDM is to arrange the velocity vector so that it points in the same direction as the trend of the trajectories with the fast-evolving components discarded. The way to accomplish this suggested by Maas and Pope is to find the space (call it $\mathcal{S}$) that is orthogonal to the long-term trajectories and then find the velocity vectors at certain points that are exactly orthogonal to $\mathcal{S}$. The key here is to find the subspace that is orthogonal to the subspace spanned by the slow eigenspace. In a Schur decomposition and after Givens rotation, the first k columns span the slow eigenspace; the rest of the $n-k$ columns are orthogonal to the first k columns. Therefore, the subspace spanned by the last $n-k$ columns is $\mathcal{S}$. If the Givens rotation were arranged in the opposite order, the slow eigenspace is not necessarily spanned by any combination of columns of $\mathbf{Q}$.

After Schur decomposition and Givens rotation, the next step is to let the velocity vector be orthogonal to $\mathcal{S}$. If a vector is orthogonal to a space, this vector must be orthogonal to all the basis vectors; and *vice versa.* The goal here is to make the velocity vector orthogonal to the last $n-k$ columns of $\mathbf{Q}$. The sufficient and necessary condition for 2 vectors to be orthogonal is to make sure their dot product is zero. For two matrices:

$$v_1 \cdot v_2 = v_1^T v_2.$$

Therefore, calculating the dot products of the velocity vector with every one of the last $n-k$ columns of $\mathbf{Q}$ is equivalent to calculating the products of the velocity vector with the last $n-k$ rows of $\mathbf{Q^H}$:

$$\begin{bmatrix} q^H_{k+1,1} & \cdots & q^H_{k+1,n} \\ \vdots & \ddots & \vdots \\ q^H_{n,1} & \cdots & q^H_{n,n} \end{bmatrix} \begin{bmatrix} v_1 \\ \vdots \\ v_n \end{bmatrix} = \begin{bmatrix} 0 \\ \vdots \\ 0 \end{bmatrix}. \tag{2.6}$$

Both $\mathbf{Q}$ and $\mathbf{v}$ depend on the position in phase space so that only some specific points have the coordinates that satisfy equation (2.6). These points are the approximated slow manifold. The manifold is only approximated because the Taylor expansion is truncated.

While ILDM is an ingenious way to expose various levels of slow manifold, it is computationally expensive to apply, primarily because of the calculation of eigenvalues and eigenvectors for each chosen point in the phase space. We present here a method that applies the same level of approximation but avoids the time-consuming eigen-decomposition steps. This method is called *Functional Equation Truncation* (FET) and will be introduced in the next chapter.

Chapter 3

Functional Equation Truncation Method

FET, like classical ILDM, can be applied to n-dimensional systems (n being any natural number) to find an approximation to the k-dimensional slow manifold ($k < n$). To show how FET works, it's best to start with $n = 2$, the simplest class of systems, and $k = 1$. Systems with higher n will be examined next and eventually a general form of FET can be developed for any n and k, provided $k < n$.

3.1 One-dimensional slow manifold in a planar system

An autonomous planar system can be written, in general, as

$$\frac{dx}{dt} = f_1(x, y), \tag{3.1a}$$

$$\frac{dy}{dt} = f_2(x, y). \tag{3.1b}$$

A slow manifold is a one-dimensional curve in a two-dimensional phase space spanned by the x and y axes. The slow manifold function should have two variables: x and y. Let us

parameterize y as a function of x:

$$y = y(x).$$

Then apply the chain rule to it so that

$$\frac{dy}{dt} = \frac{dy}{dx}\frac{dx}{dt}. \tag{3.2}$$

Equation (3.2) contains the left-hand sides (LHS) of equations (3.1). Substitute the right-hand sides (RHS) of equations (3.1) into equation (3.2) to obtain

$$f_2(x, y) = f_1(x, y)\frac{dy}{dx} \tag{3.3}$$

which has two unknowns (y and dy/dx) for each given x. (Since x is the independent variable in the equation $y = y(x)$, it is not considered to be an unknown.) This equation is called the *functional equation.*

With the functional equation, there are two unknowns and only one equation. The iterative method discussed by Fraser and Nguyen [7, 22] can be used to deal with this problem. The drawbacks of this approach are its computational expense and dependence on reasonably good initial guesses. FET is designed to calculate the initial guess in a more efficient way. Its algorithm follows.

Let the functional equation be further differentiated with respect to x. The result is

$$f_2'(x, y) = y'' f_1(x, y) + y' f_1'(x, y), \tag{3.4}$$

where the primes are used to denote total derivatives with respect to x so that

$$y'' = \frac{d^2y}{dx^2}, \tag{3.5a}$$

$$f_1'(x, y) = \frac{df_1(x, y)}{dx} = \frac{\partial f_1(x, y)}{\partial x} + \frac{\partial f_1(x, y)}{\partial y}y', \tag{3.5b}$$

$$f_2'(x, y) = \frac{df_2(x, y)}{dx} = \frac{\partial f_2(x, y)}{\partial x} + \frac{\partial f_2(x, y)}{\partial y}y'. \tag{3.5c}$$

Equation (3.4) is independent of the functional equation, and has increased the number of independent equations by one. However, in the process of obtaining equation (3.4), another variable, y'', is created, leaving the number of equations still short by one. Equation (3.4) can be further differentiated to create more independent equations but it won't be long before one realizes that the shortage will never be eliminated. Since increasing the number of equations does not work so well, the alternative is to cut the number of unknowns that need to be solved for.

According to Kaper and Kaper [13], the approximation that the classical ILDM method makes in approximating the slow manifold is to locally linearize the system by neglecting the curvature. With that being done to equation (3.4) (in other words, assuming the second- and higher-order derivatives are negligible), it becomes

$$y' f_1'(x, y) = f_2'(x, y), \tag{3.6}$$

with f_1' and f_2' given in equations (3.5). Equation (3.6) is called the *truncated* equation. At this point, for each independent x, there are two unknowns: y and y'; there are two independent equations as well: equations (3.3) and (3.6). It is now possible to plot a one-dimensional curve in the two-dimensional space defined by x and y.

3.2 One-dimensional manifold of a multi-dimensional system

Consider a system that contains n equations with n variables governed by equations of the general form:

$$\begin{aligned} \dot{y}_1 &= f_1(y_1, y_2, ..., y_n), \\ \dot{y}_2 &= f_2(y_1, y_2, ..., y_n), \\ &\vdots \\ \dot{y}_n &= f_n(y_1, y_2, ..., y_n). \end{aligned}$$

Without loss of generality, let y_n be the parameterizing variable. In this case, each variable from y_1 to y_{n-1} can be written as

$$y_m = y_m(y_n) \tag{3.7}$$

where $1 \leq m < n$. Then differentiate each parameterized variable with respect to t to get

$$\frac{dy_m}{dy_n}\dot{y}_n = \dot{y}_m.$$

Replace each time derivative with the explicit form from the original ODEs and the result is

$$f_n(y_1, y_2, ..., y_n)\frac{dy_1}{dy_n} = f_1(y_1, y_2, ..., y_n), \tag{3.8a}$$

$$f_n(y_1, y_2, ..., y_n)\frac{dy_2}{dy_n} = f_2(y_1, y_2, ..., y_n), \tag{3.8b}$$

$$\vdots$$

$$f_n(y_1, y_2, ..., y_n)\frac{dy_{n-1}}{dy_n} = f_{n-1}(y_1, y_2, ..., y_n). \tag{3.8c}$$

Differentiate both sides of each equation with respect to y_n (use f_k to denote $f_k(y_1, y_2, ..., y_n)$ where $1 \leq k \leq n$):

$$\begin{aligned}
f_n \frac{d^2 y_1}{dy_n^2} + \frac{dy_1}{dy_n}\left[\frac{\partial f_n}{\partial y_n} + \sum_{i=1}^{n-1} \frac{\partial f_n}{\partial y_i}\frac{dy_i}{dy_n}\right] &= \frac{\partial f_1}{\partial y_n} + \sum_{i=1}^{n-1} \frac{\partial f_1}{\partial y_i}\frac{dy_i}{dy_n}, \\
f_n \frac{d^2 y_2}{dy_n^2} + \frac{dy_2}{dy_n}\left[\frac{\partial f_n}{\partial y_n} + \sum_{i=1}^{n-1} \frac{\partial f_n}{\partial y_i}\frac{dy_i}{dy_n}\right] &= \frac{\partial f_2}{\partial y_n} + \sum_{i=1}^{n-1} \frac{\partial f_2}{\partial y_i}\frac{dy_i}{dy_n}, \\
&\vdots \\
f_n \frac{d^2 y_{n-1}}{dy_n^2} + \frac{dy_{n-1}}{dy_n}\left[\frac{\partial f_n}{\partial y_n} + \sum_{i=1}^{n-1} \frac{\partial f_n}{\partial y_i}\frac{dy_i}{dy_n}\right] &= \frac{\partial f_{n-1}}{\partial y_n} + \sum_{i=1}^{n-1} \frac{\partial f_{n-1}}{\partial y_i}\frac{dy_i}{dy_n}.
\end{aligned}$$

Assume the derivatives of second and higher orders are negligible and the system becomes:

$$\frac{dy_1}{dy_n}\left[\frac{\partial f_n}{\partial y_n} + \sum_{i=1}^{n-1} \frac{\partial f_n}{\partial y_i}\frac{dy_i}{dy_n}\right] = \frac{\partial f_1}{\partial y_n} + \sum_{i=1}^{n-1} \frac{\partial f_1}{\partial y_i}\frac{dy_i}{dy_n}, \tag{3.9a}$$

$$\frac{dy_2}{dy_n}\left[\frac{\partial f_n}{\partial y_n} + \sum_{i=1}^{n-1} \frac{\partial f_n}{\partial y_i}\frac{dy_i}{dy_n}\right] = \frac{\partial f_2}{\partial y_n} + \sum_{i=1}^{n-1} \frac{\partial f_2}{\partial y_i}\frac{dy_i}{dy_n}, \tag{3.9b}$$

$$\vdots$$

$$\frac{dy_{n-1}}{dy_n}\left[\frac{\partial f_n}{\partial y_n} + \sum_{i=1}^{n-1} \frac{\partial f_n}{\partial y_i}\frac{dy_i}{dy_n}\right] = \frac{\partial f_{n-1}}{\partial y_n} + \sum_{i=1}^{n-1} \frac{\partial f_{n-1}}{\partial y_i}\frac{dy_i}{dy_n}. \tag{3.9c}$$

With the combination of equations (3.8) and (3.9), there are $2(n-1)$ equations with $2(n-1)$ unknowns.

3.3 Multi-dimensional manifold of a multi-dimensional system

Suppose that the system is n-dimensional and that we want to find a p-dimensional manifold. At least locally, a manifold is the graph of a function [27]. Suppose $\mathbf{z}$ is the vector containing all the species concentrations. Partition $\mathbf{z}$ into $(\mathbf{y}, \mathbf{x})$ where $\mathbf{y}$ is an $(n-p)$-vector of dependent variables and $\mathbf{x}$ is a p-vector of independent variables. If this partitioning is

appropriately chosen, it should be possible to parameterize $\mathbf{y}$ by $\mathbf{x}$, i.e. to write $y_i = y_i(x_1, x_2, ..., x_p)$. Apply the chain rule:

$$\dot{y}_i = \frac{dy_i}{dt} = \sum_{k=1}^{p} \frac{\partial y_i}{\partial x_k} \frac{dx_k}{dt}. \tag{3.10}$$

Since there are $n - p$ y's, there will be $n - p$ equations like the one above. Then take derivatives of each of the equations with respect to each of the x_j's:

$$\begin{aligned} &\frac{\partial \dot{y}_i}{\partial x_j} + \sum_{k=1}^{n-p} \frac{\partial \dot{y}_i}{\partial y_k} \frac{\partial y_k}{\partial x_j} \\ &= \sum_{k=1}^{p} \left[\frac{\partial^2 y_i}{\partial x_k \partial x_j} \dot{x}_k + \frac{\partial y_i}{\partial x_k} \left(\frac{\partial \dot{x}_k}{\partial x_j} + \sum_{m=1}^{n-p} \frac{\partial \dot{x}_k}{\partial y_m} \frac{\partial y_m}{\partial x_j} \right) \right]. \end{aligned} \tag{3.11}$$

There will be one equation like the one above for each pair of y and x. Therefore, there are $(n - p)p$ equations. With the second derivatives in equation (3.11)

$$\left(\frac{\partial^2 y_i}{\partial x_k \partial x_j} \right)$$

discarded, the FET approximation is:

$$\frac{\partial \dot{y}_i}{\partial x_j} + \sum_{k=1}^{n-p} \frac{\partial \dot{y}_i}{\partial y_k} \frac{\partial y_k}{\partial x_j} = \sum_{k=1}^{p} \frac{\partial y_i}{\partial x_k} \left(\frac{\partial \dot{x}_k}{\partial x_j} + \sum_{m=1}^{n-p} \frac{\partial \dot{x}_k}{\partial y_m} \frac{\partial y_m}{\partial x_j} \right). \tag{3.12}$$

At this point, there are in total $n - p + (n - p)p$ equations. The number of unknowns is the same because all the y's are unknown and there are $(n - p)p$ additional ones—namely the derivatives $\frac{\partial y_i}{\partial x_k}$.

The rules for splitting dependent and independent variables are:

1. Try to avoid asymptotes. Ensure that no chosen value of an independent variable can make any of the corresponding dependent variables $\pm\infty$.

2. Quantities that can be easily measured are preferred as independent variables. If the model is used to guide experiments, we want experimental data to be used as chosen values of the independent variables.

Chapter 4

Two-dimensional system results from FET

4.1 Davis and Skodje's system

The majority of non-linear systems cannot be solved analytically. That's why model simulation and reduction methods are necessary. However, to test how close the results from model reduction methods are to the real solution, test systems can be designed which have an analytical solution for the slow manifold. One such system has been introduced by Davis and Skodje [4]:

$$\dot{x} = -x, \tag{4.1a}$$

$$\dot{y} = -\gamma y + \frac{(\gamma - 1)x + \gamma x^2}{(1 + x)^2}. \tag{4.1b}$$

where $\gamma > 1$.

Let us first calculate the exact slow manifold.

4.1.1 Analytical slow manifold

Equation (4.1a) can be solved with one of the methods that solve linear differential equations and the solution is

$$x = x_0 e^{-t}, \tag{4.2}$$

where x_0 is a constant and depends on the initial condition. To integrate equation (4.1b), the Method of Integration Factor needs to be reviewed.

Suppose a system is written, in a general case, as

$$\frac{dy}{dt} + p(t)y = g(t). \tag{4.3}$$

Multiply both sides of this equation by μ, which is a function of t, to obtain

$$\mu\frac{dy}{dt} + \mu p(t)y = \mu g(t). \tag{4.4}$$

The reason for μ is so that the LHS of equation (4.3) can be written as a derivative form:

$$\frac{d}{dt}(\mu y) = \mu g(t). \tag{4.5}$$

To ensure that equation (4.4) and equation (4.5) are the same, μ has to satisfy

$$\dot{\mu} = p(t)\mu,$$

which can be easily solved to yield

$$\mu = e^{\int p(t)dt}. \tag{4.6}$$

Equation (4.5), with both sides integrated with respect to dt, becomes

$$\mu y = \int (\mu g(t))dt + C,$$

where C is another constant. Substitute equation (4.6) into it to obtain the general solution for y:

$$y = e^{-\int p(t)dt}\left[\int (e^{\int^t p(t')dt'} g(t))dt + c_3\right]. \tag{4.7}$$

To relate the general solution to the system of interest,

$$p(t) = \gamma, \tag{4.8a}$$

$$g(t) = \frac{(\gamma - 1)x + \gamma x^2}{(x+1)^2}, \tag{4.8b}$$

Then split $g(t)$ into two parts. Substitute equation (4.2) into it to replace x:

$$g(t) = \gamma \frac{x_0 e^{-t}}{1 + x_0 e^{-t}} - \frac{x_0 e^{-t}}{(1 + x_0 e^{-t})^2}.$$

Equation (4.6) can be transformed once equations (4.8) are substituted into it. Let's look at the difficult part of the equation:

$$\int (e^{\int^t p(t')dt'} g(t))dt = \int (e^{\gamma t}(\gamma \frac{x_0 e^{-t}}{1 + x_0 e^{-t}} - \frac{x_0 e^{-t}}{(1 + x_0 e^{-t})^2}))dt.$$

Performing the integral, one finds that it equals exactly

$$\frac{x_0 e^{-t}}{1 + x_0 e^{-t}} e^{\gamma t}.$$

For the obvious part of equation (4.6),

$$e^{-\int p(t)dt} = e^{-\gamma t}.$$

With the parts solved, equation (4.6) is written as

$$y = \frac{x_0 e^{-t}}{1 + x_0 e^{-t}} + c_3 e^{-\gamma t}. \tag{4.9}$$

A slow manifold is the solution of a system with the fast-relaxing part discarded. Therefore, equation (4.9) needs to be separated into parts according to their relaxation rates. Since $\gamma > 1$, the second part decays faster than the first part and the slow manifold is

$$y = \frac{x_0 e^{-t}}{1 + x_0 e^{-t}}.$$

Because

$$x = x_0 e^{-t},$$

the analytical slow manifold becomes

$$y = \frac{x}{1+x}. \tag{4.10}$$

4.1.2 FET solution

Let us now follow the FET procedure described in section (3.1) to calculate an approximate slow manifold.

Divide equation (4.1b) by equation (4.1a) to obtain the functional equation

$$xy' = \gamma y - \frac{(\gamma-1)x + \gamma x^2}{(1+x)^2}. \tag{4.11}$$

Differentiate both sides of it with respect to x to get

$$y' + xy'' = \gamma y' - \frac{\gamma + \gamma x - 1 + x}{(1+x)^3}.$$

Let $y'' = 0$ so that it becomes the truncated equation:

$$y' = \gamma y' - \frac{\gamma + \gamma x - 1 + x}{(1+x)^3}. \tag{4.12}$$

With equations (4.11) and (4.12) combined, y' can be eliminated and the result is an equation with only x and y:

$$y(x) = \frac{x}{1+x} + \frac{2x^2}{\gamma(\gamma-1)(1+x)^3}. \tag{4.13}$$

This is the FET approximation to the slow manifold and it is exactly the same as that obtained from the classical ILDM method [4,19]. To compare it with the exact slow manifold, Figure (4.1) is shown which contains equation (4.13) and (4.10) as well as the trajectories plotted using numerical integration methods. As we can see, the approximate results are very close to the true slow manifold, and the trajectories appear to be attracted to them.

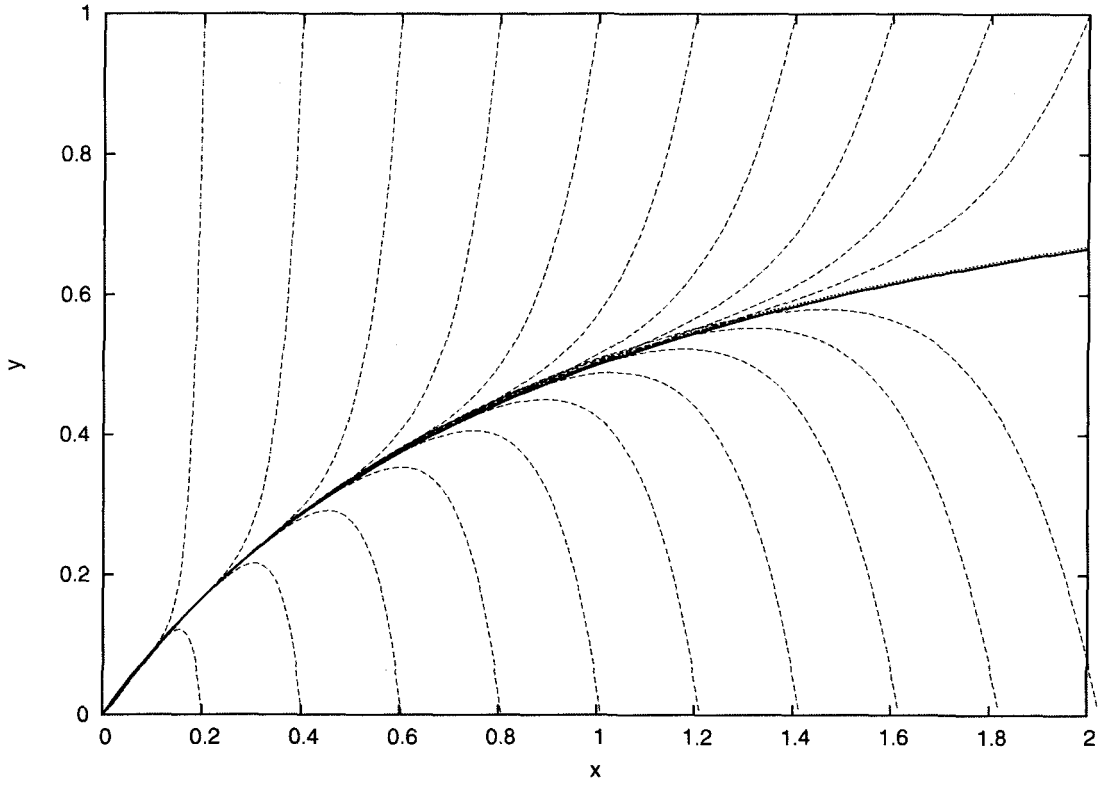

Figure 4.1: Evolution of trajectories (dashed lines) defined by the system of equations (4.1) starting from 20 different initial points, with $\gamma = 10.0$. The bold solid line in the center is the exact slow manifold. The calculated ILDM, represented by equation (4.13), is the dotted line which is slightly above the solid line and is hard to see because it is very close to the slow manifold.

4.2 Michaelis-Menten system

As mentioned in Chapter (1), the Michaelis-Menten system is

$$\dot{S} = -k_1(E_0 - C)S + k_{-1}C,$$

$$\dot{C} = k_1(E_0 - C)S - k_2C - k_{-1}C.$$

By defining

$$s = \frac{k_1 S}{k_{-1}+k_{-2}}, \quad c = \frac{C}{E_0}, \qquad \tau = k_1 E_0 t,$$

$$\alpha = \frac{k_{-1}}{k_{-1}+k_{-2}}, \quad \epsilon = \frac{k_1 E_0}{k_{-1}+k_{-2}},$$

the system becomes

$$\dot{s} = -s(1-c) + \alpha c, \tag{4.14a}$$

$$\dot{c} = \frac{s(1-c) - c}{\epsilon}, \tag{4.14b}$$

where $\dot{s} = ds/d\tau$ and $\dot{c} = dc/d\tau$. Note that some of the symbols used here are previously used in section (1.3) but they don't necessarily denote the same thing. The evolution of trajectories generated by numerical simulation methods is shown in figure (4.2)

Let c be parameterized as a function of s: $c = c(s)$ so that

$$\frac{dc}{d\tau} = \frac{dc}{ds}\frac{ds}{d\tau},$$

which is, in another form,

$$\dot{c} = c'\dot{s}, \tag{4.15}$$

where $c' = dc/ds$. By substituting $\dot{s}$ and $\dot{c}$ from equations (4.14) into equation (4.15), we can obtain the functional equation:

$$\epsilon[-s(1-c) + \alpha c]c' = s(1-c) - c. \tag{4.16}$$

Differentiate both sides of equation (4.16) with respect to s to get

$$(sc' + \alpha c' + c - 1)c' + [\alpha c - s(1-c)]\,c'' = \frac{1 - c - sc' - c'}{\epsilon}. \tag{4.17}$$

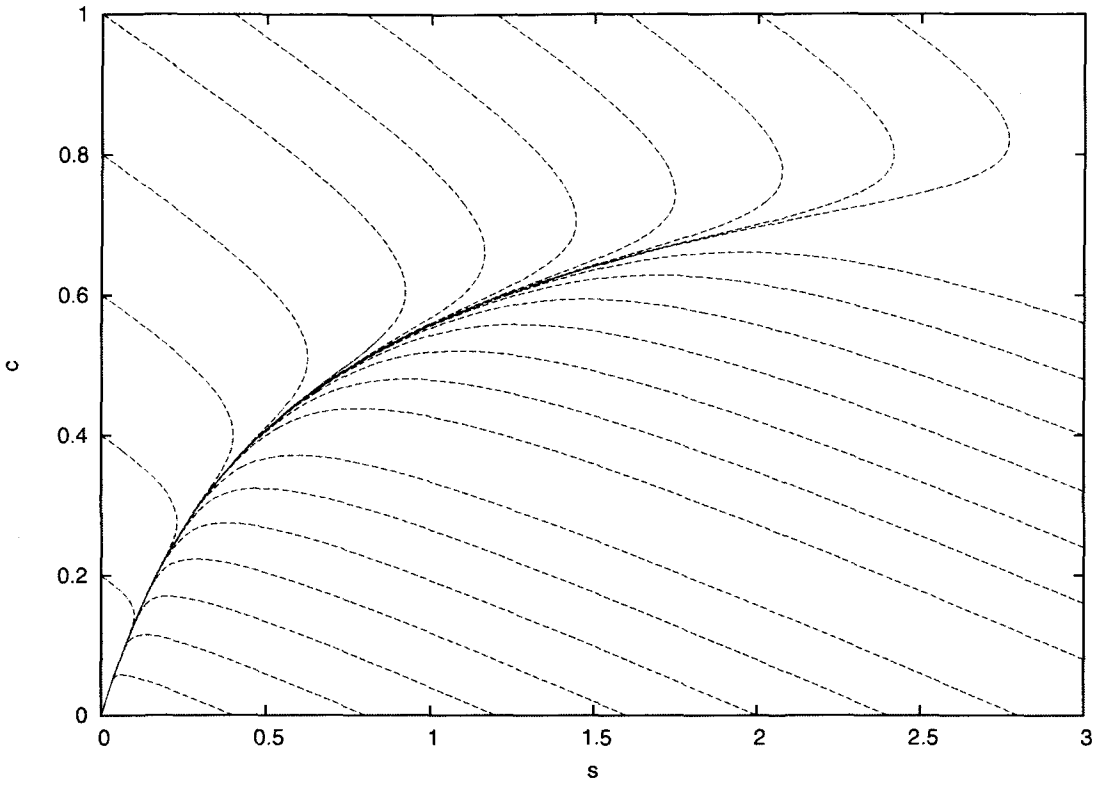

Figure 4.2: The trajectories governed by the two-dimensional Michaelis-Menten system as in equations (4.14) with the coefficients being $\alpha = 0.6$ and $\epsilon = 5$. The trajectories are shown as dashed lines and each point where a trajectory meets the axes is its initial condition. Note that the trajectories tend to converge toward a central curve, which is the slow manifold we wish to approximate.

By assuming $c'' = 0$, we can transform equation (4.17) into the truncated equation:

$$(sc' + \alpha c' + c - 1)c' = \frac{1 - c - sc' - c'}{\epsilon}. \tag{4.18}$$

With equations (4.16) and (4.18) combined, c' can be eliminated so that for each chosen s, there is a corresponding c. These equations are solved numerically to yield the approximate slow manifold shown in figure (4.3).

Figure (4.4) contains the approximated slow manifold together with the trajectories. It shows that the approximate slow manifold is close to exact.

4.3 Lindemann Mechanism

As another example, the Lindemann mechanism will be examined in this section. This mechanism was first proposed by F. A. Lindemann in 1922 [18] and it represents chemical reactions that have the general form

$$A + A \underset{k_{-1}}{\overset{k_1}{\rightleftharpoons}} A + B,$$
$$B \underset{k_{-2}}{\overset{k_2}{\rightleftharpoons}} P,$$

where A is the reactant, B is the energized form of A, and P is the product. With the same letter denoting both the chemical species and its concentration, the rate equations for this mechanism are

$$\frac{dA}{dt} = -k_1 A^2 + k_{-1} AB, \tag{4.19a}$$
$$\frac{dB}{dt} = k_1 A^2 - k_{-1} AB - k_2 B + k_{-2} P, \tag{4.19b}$$
$$\frac{dP}{dt} = k_2 B - k_{-2} P. \tag{4.19c}$$

There is also a mass-conservation equation:

$$A + B + P = A_0, \tag{4.20}$$

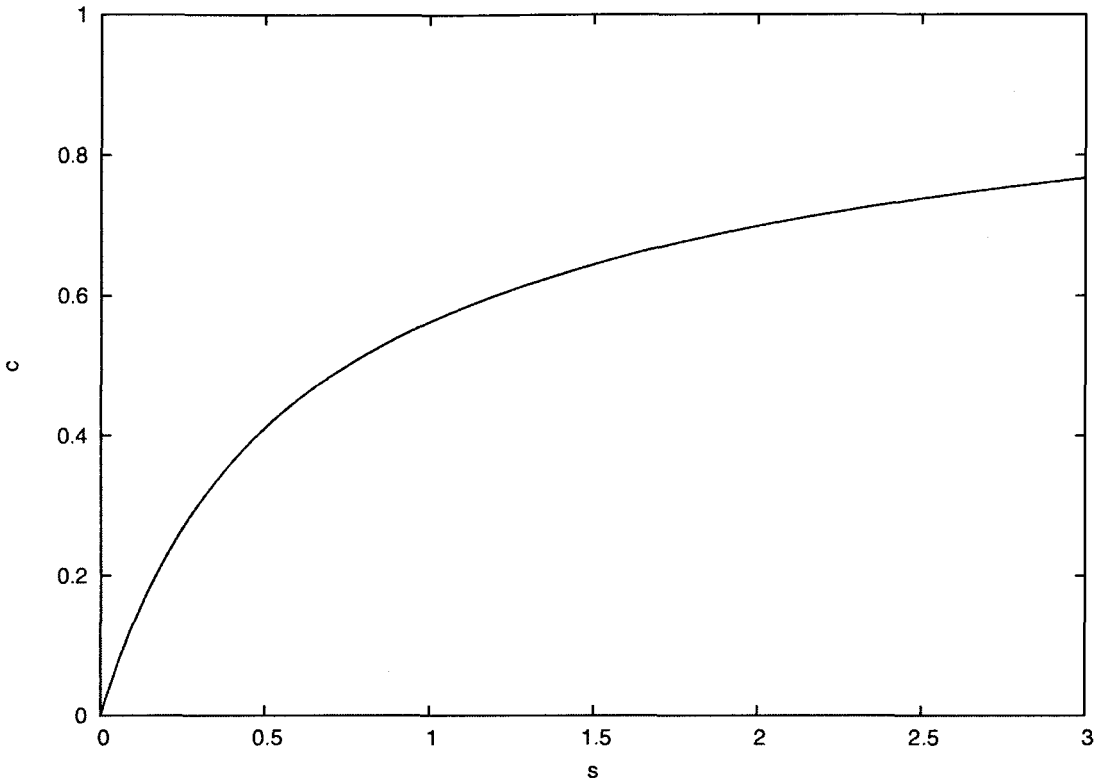

Figure 4.3: The plot of the FET approximation (solid line), as well as the ILDM approximation (dashed line), to the slow manifold for the Michaelis-Menten system. The values for the coefficients are: $\alpha = 0.6$ and $\epsilon = 5$. Note that the dotted line cannot be seen because results from these two methods are too close to each other (if not identical) and they overlap.

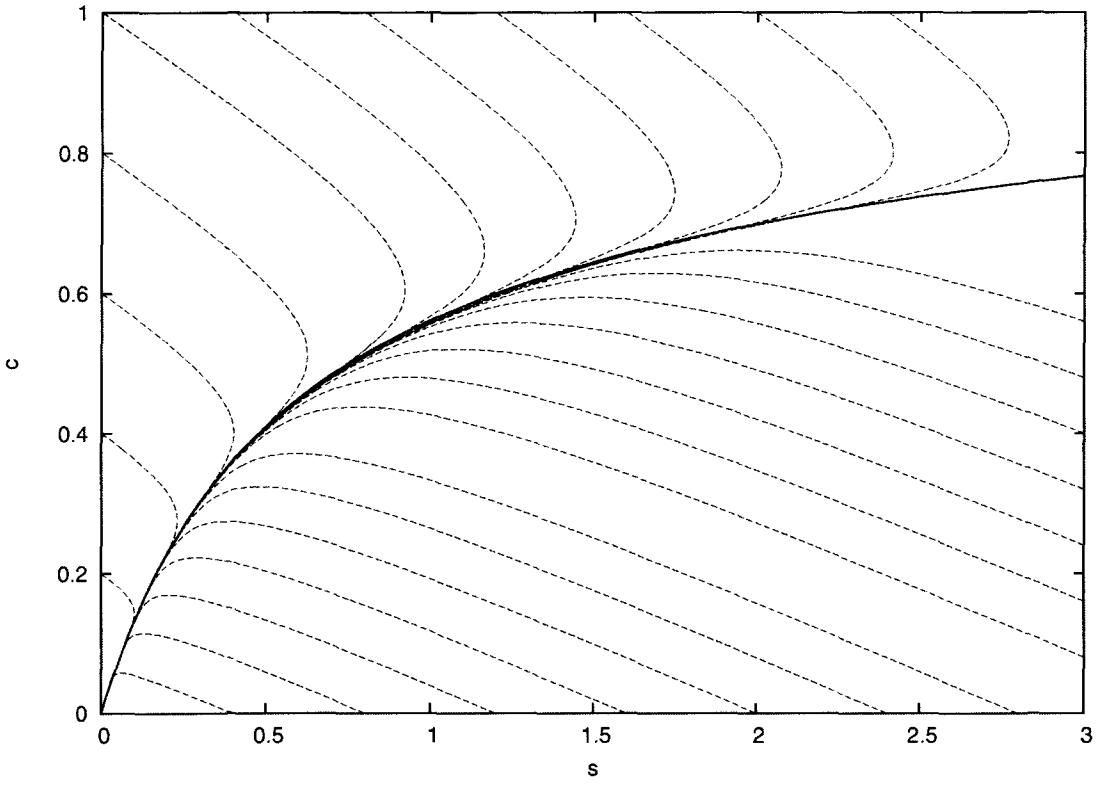

Figure 4.4: The combination of figures (4.2) and (4.3). The dashed lines are the trajectories and the solid line is the approximate slow manifold computed by both FET and classical ILDM methods. The coefficient values are still $\alpha = 0.6$ and $\epsilon = 5$. Notice that, again, the trajectories tend to converge toward the slow manifold, and the approximate slow manifold is very close to it.

where A_0 is the initial value of A, and the initial B and P are both 0, which is often how this kind of reaction is started. By applying equation (4.20) to the rate equations (4.19), they can be simplified to omit equation (4.19c). To non-dimensionalize the system, we define the following variables and coefficients:

$$a = \frac{k_1 A}{k_2}, \quad b = \frac{k_1 B}{k_2}, \quad \tau = k_2 t,$$
$$\alpha = \frac{k_{-1}}{k_1}, \quad \beta = \frac{k_{-2}}{k_2}, \quad a_0 = \frac{k_1 A_0}{k_2},$$

and equation (4.19) can be rewritten as

$$\dot{a} = -a^2 + \alpha a b, \tag{4.21a}$$

$$\dot{b} = a^2 - \alpha a b - b + \beta(a_0 - a - b). \tag{4.21b}$$

The phase-portrait of this non-dimensionalized system is shown in figure (4.5). Notice that because we treat this system as being fully reversible, the equilibrium point is not at the origin.

To compute the FET approximation of the slow manifold, let b be parameterized by a. Its time derivative is

$$\dot{b} = b'\dot{a}. \tag{4.22}$$

By substituting $\dot{b}$ and $\dot{a}$ from equations (4.21) into equation (4.22), we obtain the functional equation:

$$a^2 - \alpha a b - b + \beta(a_0 - a - b) = b'(-a^2 + \alpha a b). \tag{4.23}$$

Differentiate both sides of equation (4.23) with respect to a to get

$$2a - \alpha(b + ab') - b' + \beta(-1 - b') = b''(-a + \alpha a b) + b'[-2a + \alpha(b + ab')].$$

The truncated equation is obtained by assuming $b'' = 0$:

$$2a - \alpha(b + ab') - b' + \beta(-1 - b') = b'[-2a + \alpha(b + ab')]. \tag{4.24}$$

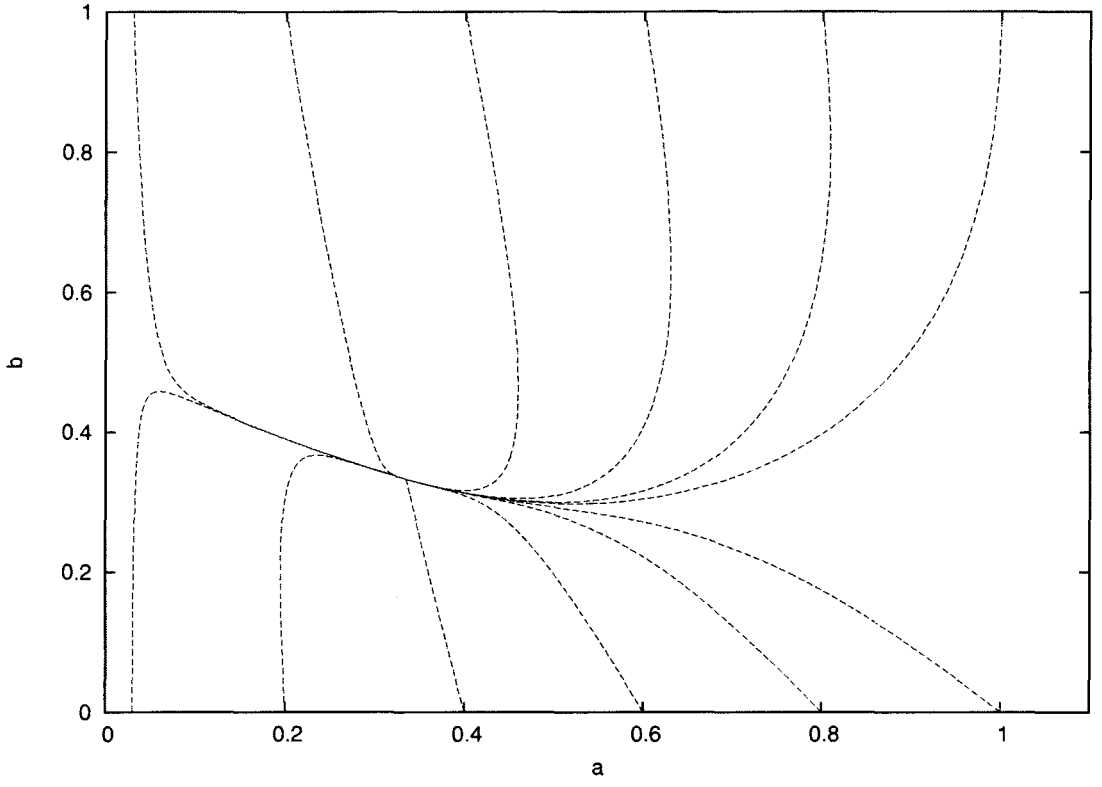

Figure 4.5: The evolution of trajectories starting from different initial points. They appear to converge first to a one-dimensional curve (the slow manifold) before eventually approaching the equilibrium point. The coefficients are chosen to be $\alpha = \beta = a_0 = 1$.

By combining equations (4.23) and (4.24) to eliminate b', we get the approximate slow manifold which is shown in figure (4.6). Figure (4.7) is shown in order to compare the trajectories with the approximate slow manifold. It is merely a combination of figures (4.5) and (4.6). The trajectories tend to converge to the approximate slow manifolds and approach the equilibrium point along it. This means the analytical results are very consistent with the numerical ones.

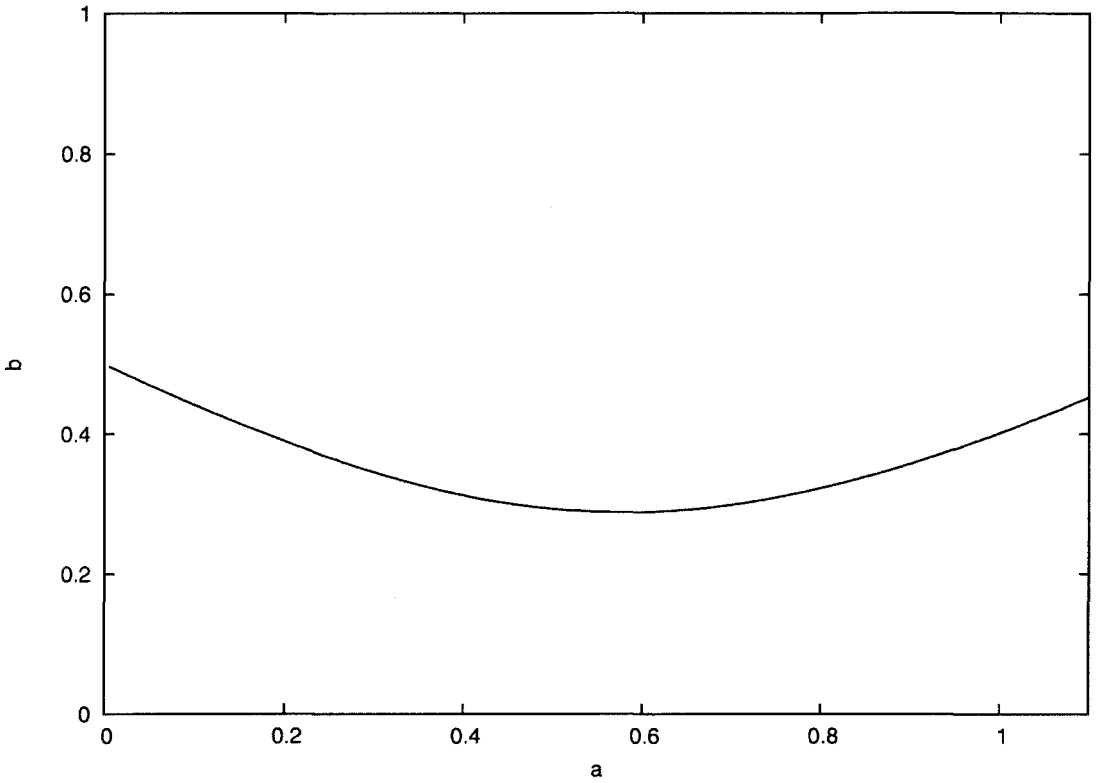

Figure 4.6: The FET-approximated slow manifold for the Lindemann mechanism (solid line). The ILDM approximation is shown as well in dotted line although they overlap with each other. The coefficients remain the same as that in figure (4.5) which is $\alpha = \beta = a_0 = 1$.

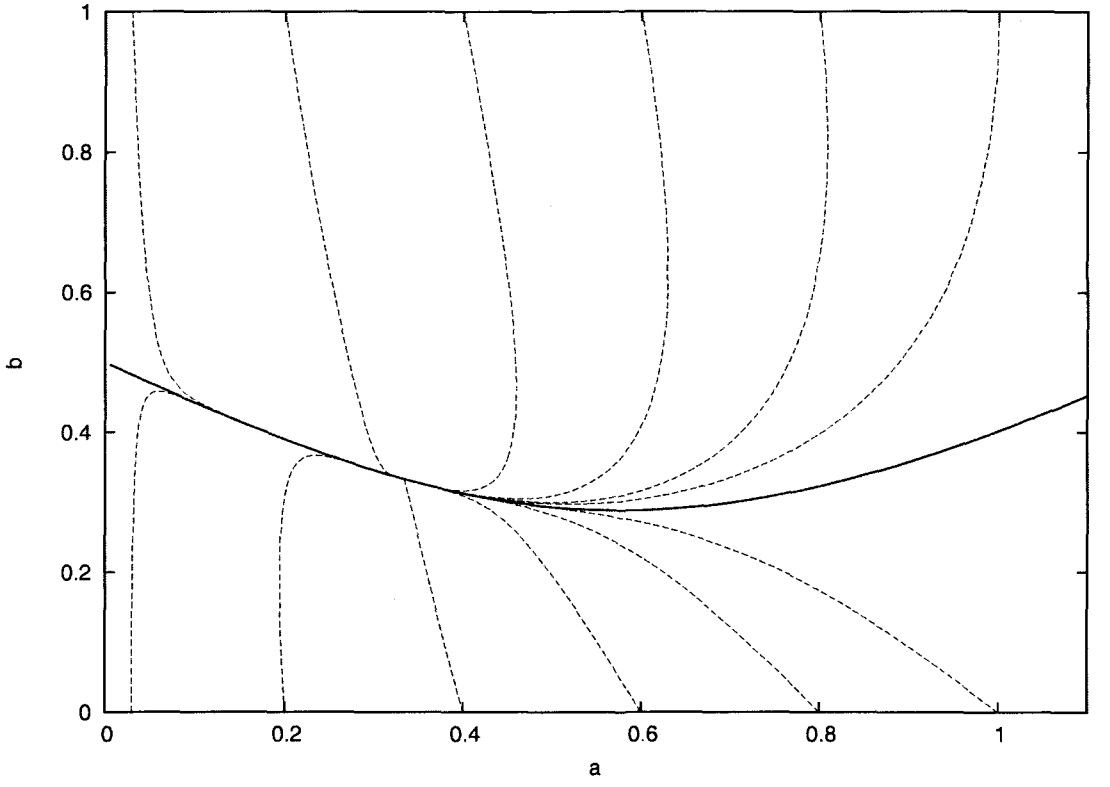

Figure 4.7: The approximate slow manifold (solid line) together with the numerically simulated trajectories (dashed lines) for the Lindemann mechanism. The coefficients are the same as those used in figures (4.5) and (4.6), i.e. $\alpha = \beta = a_0 = 1$.

Chapter 5

One-dimensional manifold of a three-dimensional system

While the slow manifold of a two-dimensional system is one-dimensional, we can have either one- or two-dimensional manifolds for a three-dimensional system. With our FET method, if only one of the three variables is chosen to be independent and the other two are parameterized with respect to it, the approximate slow manifold is one-dimensional; on the other hand, if two variables are chosen to be independent, the result is an approximation to a two-dimensional slow manifold. In this chapter, the approximation of a one-dimensional manifold is shown for the Extended Michaelis-Menten system. The results for the two-dimensional manifold of a three-dimensional system are presented in the next chapter.

5.1 Rate equations

The system used in this section is a modified version of the Michaelis-Menten mechanism from section 4.2 with one more species introduced. The mechanism is

$$E + S \underset{k_{-1}}{\overset{k_1}{\rightleftharpoons}} C \underset{k_{-2}}{\overset{k_2}{\rightleftharpoons}} F \overset{k_3}{\rightarrow} E + P.$$

The added species is F, which like the enzyme-reactant complex C, is the enzyme-product complex: $F = EP$. This mechanism is called the Extended Michaelis-Menten mechanism (EMM), and it has been previously studied [28].

The system can be modelled by five equations:

$$\dot{E} = -k_1 ES + k_{-1} C + k_3 F, \tag{5.1a}$$

$$\dot{S} = -k_1 ES + k_{-1} C, \tag{5.1b}$$

$$\dot{C} = k_1 ES - k_{-1} C - k_2 C + k_{-2} F, \tag{5.1c}$$

$$\dot{F} = k_2 C - k_{-2} F - k_3 F, \tag{5.1d}$$

$$\dot{P} = k_3 F. \tag{5.1e}$$

There are two mass-conservation equations:

$$F + E + C = E_0, \tag{5.2a}$$

$$S + C + F + P = S_0. \tag{5.2b}$$

By using the conserved masses, two equations in (5.1) can be eliminated, the remaining ones containing the same information as the complete set. The ones we chose to eliminate are equations (5.1a) and (5.1e). The other three equations can be rewritten, with E being replaced by $E_0 - F - C$ and P being replaced by $S_0 - F - C - S$, as

$$\dot{S} = -k_1 ES + k_{-1} C, \tag{5.3a}$$

$$\dot{C} = k_1 ES - k_{-1} C - k_2 C + k_{-2} F, \tag{5.3b}$$

$$\dot{F} = k_2 C - k_{-2} F - k_3 F. \tag{5.3c}$$

To non-dimensionalize equations (5.3), define

$$s = S k_1 / k_{-1}, \quad c = C/E_0, \qquad f = F/E_0,$$

$$\tau = k_1 E_0 t, \qquad \epsilon = k_1 E_0 / k_{-1}, \quad \beta = k_2 / k_{-1},$$

$$\gamma = k_{-2}/k_{-1}, \quad \alpha = k_3/k_{-1}.$$

The transformed rate equations are

$$\dot{f} = \frac{\beta c - \gamma f - \alpha f}{\epsilon}, \tag{5.4a}$$

$$\dot{c} = \frac{s(1-f-c) - c - \beta c + \gamma f}{\epsilon}, \tag{5.4b}$$

$$\dot{s} = -s(1-f-c) + c. \tag{5.4c}$$

The dynamics of equations (5.4) is illustrated in figure (5.1).

5.2 FET implementation

To find the one-dimensional manifold, two of the variables are parameterized by the other one which is chosen to be the independent variable. In this case, s is the choice because its value can be any positive real number without making the other variables reach an asymptotic infinity. The other two variables are parameterized with respect to s: $f(s)$ and $c(s)$. The derivatives of these two dependent variables with respect to the non-dimensional time τ are

$$\dot{f} = \frac{df}{ds}\dot{s}, \tag{5.5a}$$

$$\dot{c} = \frac{dc}{ds}\dot{s}, \tag{5.5b}$$

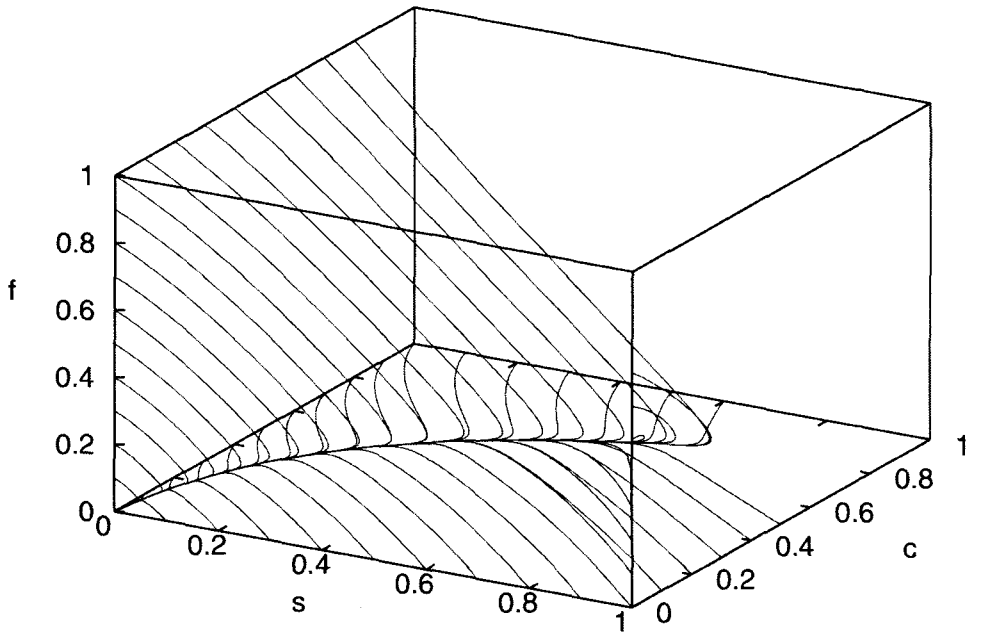

Figure 5.1: Evolution of the system defined by equations (5.4) in three-dimensional space ($\alpha = 0.1$, $\beta = 1$, $\gamma = 1$, $\epsilon = 1$). Note that all trajectories approach a central one, the one-dimensional slow manifold. The one-dimensional slow manifold lies within a two-dimensional manifold which all trajectories are attracted to before approaching the one-dimensional manifold.

where, again,

$$\frac{df}{d\tau} = \dot{f}, \qquad \frac{dc}{d\tau} = \dot{c}, \qquad \frac{ds}{d\tau} = \dot{s}.$$

Substitute equations (5.4) into equations (5.5) and the result is the set of functional equations

$$[-s(1-f-c)+c]f' = \frac{\beta c - (\gamma+\alpha)f}{\epsilon}, \tag{5.6a}$$

$$[-s(1-f-c)+c]c' = \frac{s(1-f-c) - c(1+\beta) + \gamma f}{\epsilon}. \tag{5.6b}$$

Take derivatives of both side of each equation with respect to s to obtain

$$\frac{\beta}{\epsilon}c' - \frac{\alpha+\gamma}{\epsilon}f' = f''[-s(1-f-c)+c] + f'[-1+f+c+(s+1)c'+sf'], \tag{5.7a}$$

$$\frac{1-f-c}{\epsilon} - \frac{s+1+\beta}{\epsilon}c' + \frac{\gamma-s}{\epsilon}f' = c''[-s(1-f-c)+c] + c'[-1+f+c+(s+1)c'+sf'], \tag{5.7b}$$

in which

$$f' = \frac{df}{ds} \qquad \text{and} \qquad c' = \frac{dc}{ds}.$$

Let $c'' = f'' \approx 0$ so that equations (5.7) can be transformed into the truncated equations

$$\frac{1-f-c}{\epsilon} - \frac{s+1+\beta}{\epsilon}c' + \frac{\gamma-s}{\epsilon}f' = c'[-1+f+c+(s+1)c'+sf'], \tag{5.8a}$$

$$\frac{\beta}{\epsilon}c' - \frac{\alpha+\gamma}{\epsilon}f' = f'[-1+f+c+(s+1)c'+sf']. \tag{5.8b}$$

With equations (5.6) and (5.8) combined, there are four equations. For each given s, there are four unknowns as well: f, c, c', and f'. Therefore, each s can be brought into correspondence with one or more sets of f and c values.

5.3 Solutions

To solve this set of equations, the Newton-Raphson method for solution of sets of nonlinear algebraic equations needs to be reviewed [21, 23]. Suppose the equation to be solved is

$$\mathbf{f}(\mathbf{x}) = 0,$$

where $\mathbf{f}$ and $\mathbf{x}$ are both vectors in n-dimensional space. Let x_i be the approximate root generated in step i. The Taylor expansion of $f(x)$ with respect to this point is

$$\mathbf{f(x)} \approx \mathbf{f(x_i)} + \mathbf{J}\,(\mathbf{x_i})\,[\mathbf{x} - \mathbf{x_i}]\,,$$

plus some higher order terms which we neglect. $\mathbf{J}\,(\mathbf{x_i})$ is the $n \times n$ Jacobian at x_i whose elements are defined as

$$J_{kl} = \frac{\partial f_k}{\partial x_l}.$$

Because $\mathbf{f(x)} = 0$, an improved root is obtained by solving for $\mathbf{x}_{i+1}$ in

$$0 = \mathbf{f(x_i)} + \mathbf{J}\,(\mathbf{x_i})\,[\mathbf{x_{i+1}} - \mathbf{x_i}]\,. \tag{5.9}$$

Define

$$\mathbf{x_{i+1}} - \mathbf{x_i} = \Delta\mathbf{x}.$$

Equation (5.9) becomes

$$\mathbf{J}\,(\mathbf{x_i})\,\Delta\mathbf{x} = -\mathbf{f(x_i)}.$$

This equation can be solved by mathematical software such as Maple© using

```
LinearSolve(J(xi), -f(xi))
```

or similar methods. Then $\mathbf{x_{i+1}}$ can be obtained by

$$\mathbf{x_{i+1}} = \Delta\mathbf{x} + \mathbf{x_i}$$

and the iteration process goes on.

For each s, in our case, there is a four-dimensional vector to be solved for, namely $\begin{bmatrix} f & c & f' & c' \end{bmatrix}^T$. If the s values are chosen close enough to each other, these points can be connected to form a one-dimensional curve, which is the approximate one-dimensional slow manifold and is shown in figure (5.2).

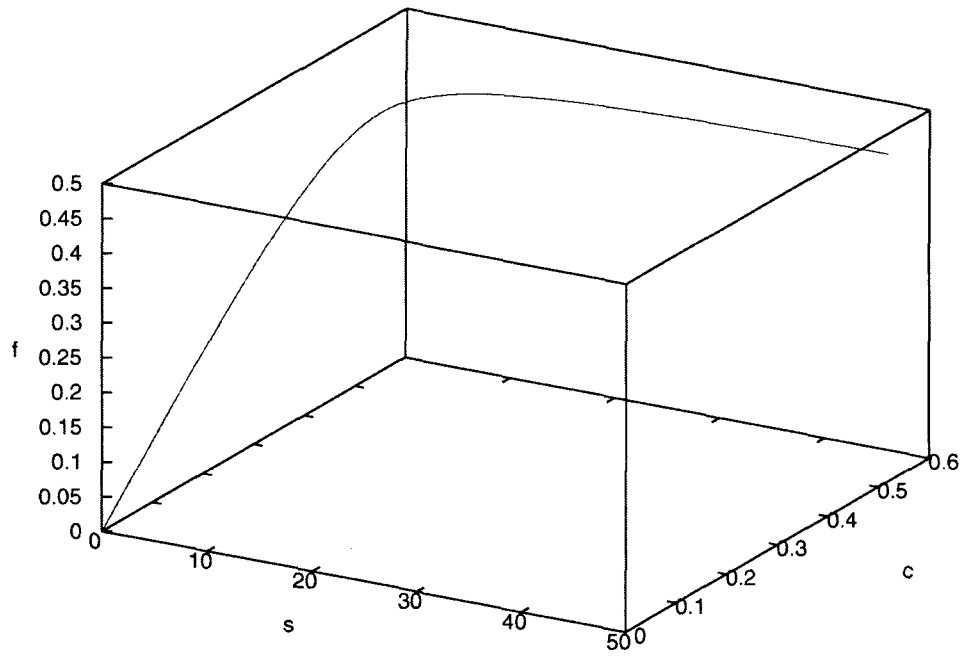

Figure 5.2: The approximated slow manifolds of the Extended Michaelis-Menten system (with parameter values $\alpha = 0.1$, $\beta = 1$, $\gamma = 1$, and $\epsilon = 1$) by both classical ILDM (dashed) and our FET method (solid). Note that the two lines are indistinguishable from each other.

The Newton-Raphson method is used for both FET and the classical ILDM methods to solve the relevant algebraic equations. The software used for the implementation is Maple. Except for the core algorithm, the rest of the numerical calculation for both methods is done with the same method. All calculations are carried out on the same computer in order to compare the computer times required by the two methods. Because the classical ILDM method requires the computation of eigenvalues of the Jacobian for each local point, it is expected to be slower than the FET method. The results agree with this conjecture. With 200 values of s chosen, it takes the ILDM method 36.46 seconds to finish the computation, whereas FET requires only 1.72 seconds.

Along with the realistic results, there can be one or more artificial manifolds obtained for each model. These manifolds represent non-physical solutions of the original system. A more detailed discussion on artificial manifolds is provided by Bykov *et al* [2]. Figure 5.3 is a plot of one such manifold for the Extended Michaelis-Menten system. This manifold can easily be distinguished from the correct slow manifold because it is not physically acceptable.

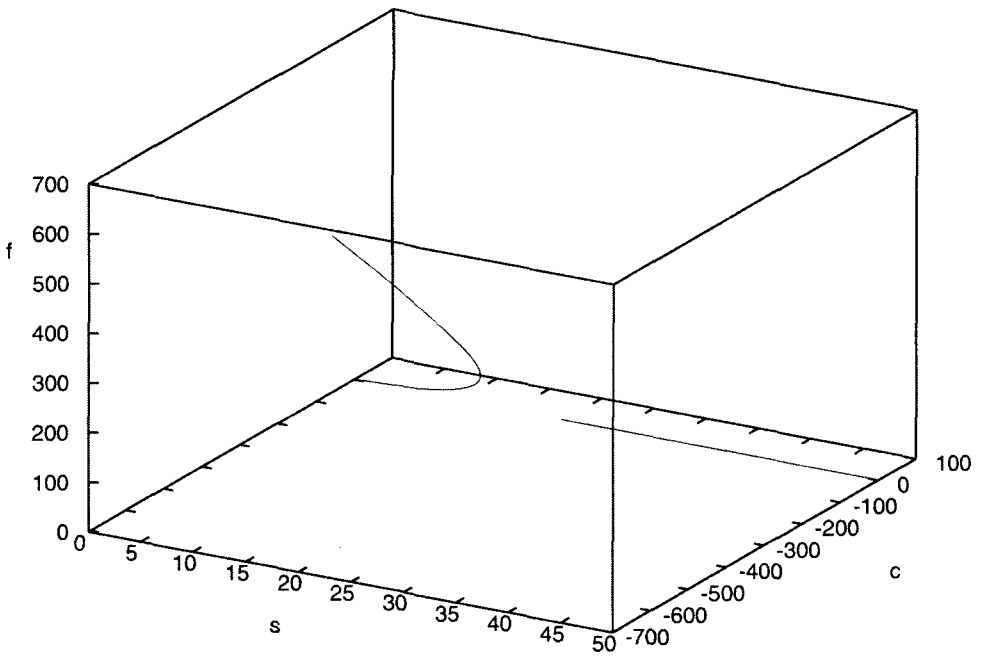

Figure 5.3: The artificial manifold computed by FET for EMM. Notice that the manifold resides on negative part of c. Since c stands for the concentration of a chemical species, its value must always be non-negative. Therefore, this manifold is unrealistic.

Chapter 6

Two-dimensional manifold of a three-dimensional system

The calculation of a two-dimensional manifold is also tested using the Extended Michaelis-Menten mechanism. Equations (5.4) are the reduced and non-dimensionalized rate equations for this mechanism. To obtain an approximation to the two-dimensional slow manifold, one of the variables is chosen to be the dependent one and the other two become the independent ones. In this case, f is the dependent one and s and c the independent ones such that f can be written as

$$f = f(s, c).$$

The derivative of the parameterized f is

$$\frac{df}{d\tau} = \frac{\partial f}{\partial c}\frac{dc}{d\tau} + \frac{\partial f}{\partial s}\frac{ds}{d\tau},$$

or, equivalently,

$$\dot{f} = \frac{\partial f}{\partial c}\dot{c} + \frac{\partial f}{\partial s}\dot{s}. \tag{6.1}$$

Substitute $\dot{f}$, $\dot{s}$, and $\dot{c}$ from equations (5.4) into equation (6.1) to get the functional equation:

$$\frac{\beta c-(\gamma+\alpha)f}{\epsilon}=\frac{\partial f}{\partial c}\left[\frac{s(1-f-c)-c(1+\beta)+\gamma f}{\epsilon}\right]+\frac{\partial f}{\partial s}\left[-s(1-f-c)+c\right]. \tag{6.2}$$

Differentiate equation (6.1) with respect to the independent variable c to obtain the independent equation

$$\frac{\partial \dot{f}}{\partial c}+\frac{\partial \dot{f}}{\partial f}\frac{\partial f}{\partial c}=\frac{\partial^2 f}{\partial c^2}\dot{c}+\frac{\partial f}{\partial c}\left(\frac{\partial \dot{c}}{\partial c}+\frac{\partial \dot{c}}{\partial f}\frac{\partial f}{\partial c}\right)+\frac{\partial^2 f}{\partial c\partial s}\dot{s}+\frac{\partial f}{\partial s}\left(\frac{\partial \dot{s}}{\partial c}+\frac{\partial \dot{s}}{\partial f}\frac{\partial f}{\partial c}\right). \tag{6.3}$$

Truncate the second-order partial derivatives in equation (6.3) to obtain the approximate equation:

$$\frac{\partial \dot{f}}{\partial c}+\frac{\partial \dot{f}}{\partial f}\frac{\partial f}{\partial c}=\frac{\partial f}{\partial c}\left(\frac{\partial \dot{c}}{\partial c}+\frac{\partial \dot{c}}{\partial f}\frac{\partial f}{\partial c}\right)+\frac{\partial f}{\partial s}\left(\frac{\partial \dot{s}}{\partial c}+\frac{\partial \dot{s}}{\partial f}\frac{\partial f}{\partial c}\right). \tag{6.4}$$

This is the general truncated equation in the process of finding the two-dimensional approximate slow manifold of a three-dimensional system. For the EMM mechanism, all the time-derivatives in equation (6.4) are replaced by equations (5.4), yielding the truncated equation

$$\frac{\beta}{\epsilon}-\frac{\gamma+\alpha}{\epsilon}\frac{\partial f}{\partial c}=\frac{\partial f}{\partial c}\left[\frac{-s-1-\beta}{\epsilon}+\frac{-s+\gamma}{\epsilon}\frac{\partial f}{\partial c}\right]+\frac{\partial f}{\partial s}\left[s+1+s\frac{\partial f}{\partial c}\right]. \tag{6.5}$$

To get the second truncated equation, let equation (6.2) be differentiated with respect to s and truncate the local curvature terms. With the intermediate steps omitted, the second truncated equation for EMM is

$$-\frac{\gamma+\alpha}{\epsilon}\frac{\partial f}{\partial s}=\frac{\partial f}{\partial c}\left[\frac{1-f-c}{\epsilon}+\frac{(-s+\gamma)}{\epsilon}\frac{\partial f}{\partial s}\right]+\frac{\partial f}{\partial s}\left[-(1-f-c)+s\frac{\partial f}{\partial s}\right]. \tag{6.6}$$

At this point, there are three equations: (6.2), (6.5), and (6.6); and three unknowns for each set of s and c: f, $\frac{\partial f}{\partial c}$, and $\frac{\partial f}{\partial s}$. The solution, plotted in a three-dimensional space defined by s, c, and f, is a surface as shown in figure (6.1). To show the accuracy and consistency of the FET method, the calculated two-dimensional surface above is compared to trajectories

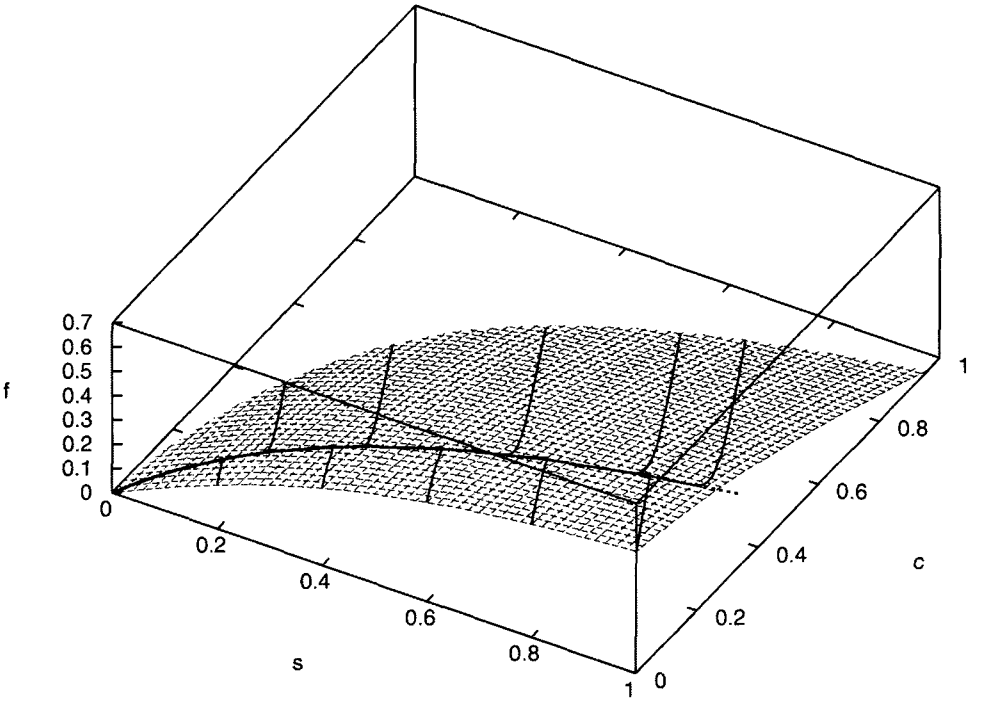

Figure 6.1: Two-dimensional FET-approximated slow manifold of the Extended Michaelis-Menten system in a three-dimensional space. The parameter values are the same as for figure (5.2), that is, $\alpha = 0.1$, $\beta = 1$, $\gamma = 1$, and $\epsilon = 1$. The grid surface is the two-dimensional slow manifold. The dotted line that runs through the surface and reaches the origin is the one-dimensional slow manifold. Additional trajectories that start on the edge of the surface are shown (solid lines converging towards the central curve). Notice that once a trajectory reaches either the one- or two- dimensional slow manifold, it does not leave it.

generated using numerical simulation as well as to the approximate one-dimensional slow manifold calculated in section (5.3).

For each point on a trajectory there are three coordinates (s, c, f). There are three coordinates (s, c, $f_a(s,c)$) associated with each point on the manifold as well, with $f_a(s,c)$ being the approximated one. The manifold is compared to one of the trajectories by calculating the relative error

$$\delta = \left| \frac{f_a(s,c) - f}{f} \right|.$$

The result is shown in figure (6.2). It shows that f and $f_a(s,c)$ diverge at first but approach each other asymptotically and eventually both reach the origin. Theoretically, the FET manifold should approach the slow manifold asymptotically as time proceeds. The reason for the divergence in figure (6.2) is that the initial point of the trajectory is chosen to be EXACTLY on the FET manifold. It is, however, the slow manifold that the trajectory is attracted to. As a consequence, it leaves the FET manifold for the slow manifold. Everything eventually comes together as a result of the FET manifold and the slow manifold approaching each other asymptotically. Notice that even at the peak of the plot in figure (6.2), the δ value is still small which means the FET surface is quite close to the slow manifold.

A similar comparison method was used between the one-dimensional and two-dimensional FET. In principle, the one-dimensional ILDM should be exactly embedded in the two-dimensional ILDM. Numerically, this appears to be true for the FET-approximated manifolds (not shown).

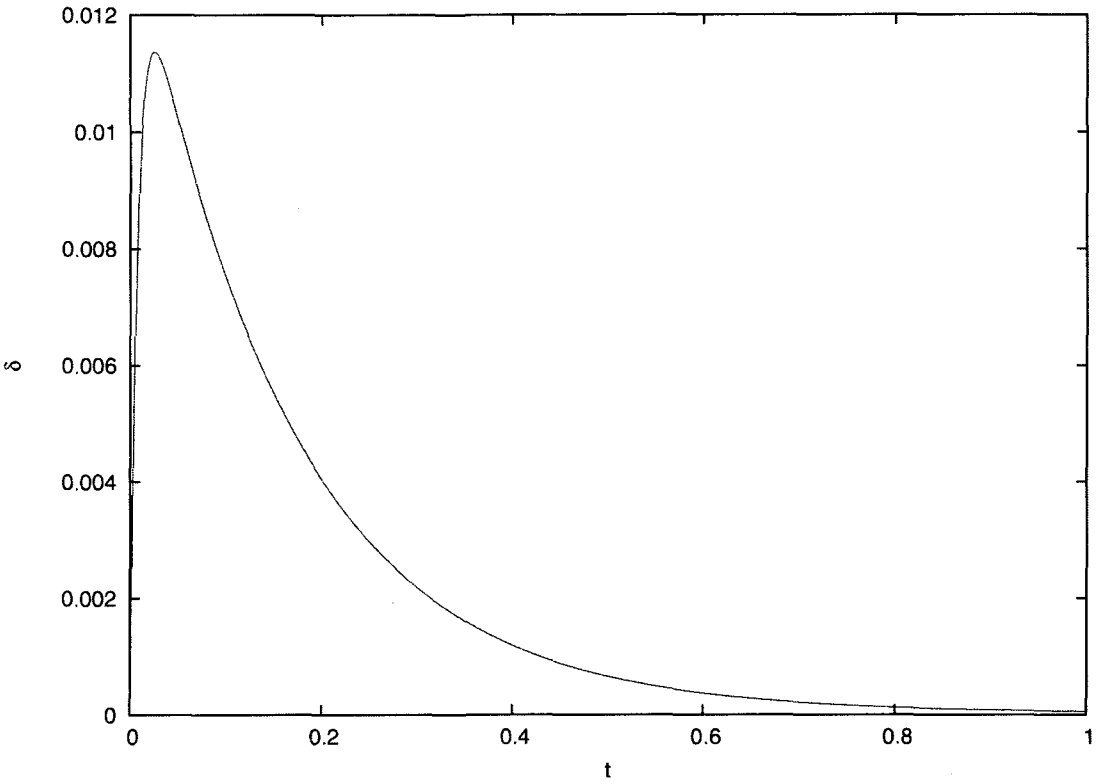

Figure 6.2: Relative error δ as a function of time. The numerical simulation is done using *xppaut* [5]. With all the parameter values being the same as for figure 6.2, the initial point is $(s, c, f) = (20, 0, 0.4820815)$ which is exactly on the two-dimensional FET surface.

Chapter 7

Discussion and Conclusion

Most closed chemical systems relax in hierarchical order eventually reaching the equilibrium point. Many model reduction methods exploit this relaxation order to discard the fast scales and obtain the slow ones. Singular perturbation is a method that relies on insights into the nature of the reaction to redefine variables so that one or more of the differential equations can be reduced to plain algebraic equation(s). With the algebraic equation(s) combined, a geometric surface (the slow manifold) can be constructed. This method is widely researched and used. However, the transformation of axes requires a great deal of analytical work for each system. Moreover, the hierarchical orders are not always obvious.

The classical ILDM method is a way to overcome both disadvantages associated with singular perturbation theory. Its implementation is largely automated and it exploits the hidden hierarchical orders which are, in many cases, difficult for the singular perturbation method to expose. However, because it involves obtaining the eigen-decomposition of the Jacobian matrix for each point along the slow manifold, the amount of computation required by this method can be enormous. For systems with high dimension, this problem can be critical.

The computational singular perturbation (CSP) method [10, 14–16] is a combination of the conventional singular perturbation method and the classical ILDM method. It uses eigen-decomposition of the Jacobian to distinguish the slow-evolving directions from the fast-evolving ones, and transforms the variables accordingly so that each new variable is parallel to one of the eigenvectors of the Jacobian before the transformation. In contrast to the conventional singular perturbation method, the calculations using CSP are done in an automatic and programmable fashion.

FET, inspired by the underlying ideas of the classical ILDM as explained by Kaper and Kaper [13], can approximate the slow manifold faster while generating results with the same degree of accuracy. It discards local curvature by algebraic means to avoid the computationally expensive calculation of eigenvalues and eigenvectors as required by both classical ILDM and CSP. The parameterization of dependent variables in terms of independent variables generates the functional equation(s) whose derivatives with respect to the independent variables, after discarding the local curvature, produces the truncated equation(s). With values assigned to the independent variables, the dependent variables can be found. For many systems, FET and classical ILDM generate approximations very close to the real ones. To get the exact slow manifold, Fraser's iterative method [7] can become the method of choice.

Fraser's method involves the iteration of the functional equation whose results after each step asymptotically approach the true slow manifold. This method, like most other iterative methods, requires an initial guess. Depending on the system, the closeness of the initial guess to the slow manifold is very important and trivial guesses are very likely to fail. FET, as well as classical ILDM, can be used as a way to obtain the initial guesses to feed into such an iterative method. Taking FET, for example, the set of equations (functional and

truncated) contains both the dependent variables and the first-order local derivatives, and all of them can be solved for given values of the independent variables. The local derivatives can be used to initialize the iterative algorithm. Davis *et al* [4, 29] have applied ILDMs as initial guess for the iterative algorithm. Depending on the number of iterative steps taken, the result can be as close as desired to the slow manifold.

These model reduction methods can be categorized based on whether or not they return "local" results. Local results are points on the slow manifold obtained from a method without the construction of the whole or a portion of the manifold. In this sense, both FET and classical ILDM methods are local; singular perturbation, CSP, and Fraser's iterative methods are not because they return the whole slow manifold as a function.

There is a way, theoretically, for the FET method to locally generate an asymptotically accurate approximation to a slow manifold. Taking equations (5.7) for example, we could choose not to truncate them to generate the truncated equations (5.8). Instead, further derivatives can be taken with respect to the independent variable (s) to produce another set of equations which has higher derivatives c''' and f'''. These third-order derivatives can be assumed 0 to give higher-order truncated equations. With two more equations and two more unknowns (c'' and f'') than before, they can still be solved, and the results in this case are theoretically more accurate than the second-order truncation. If one is still not satisfied with this degree of approximation, even higher derivatives can be taken and so on. Nonetheless, it is not applicable in practice because as the number of unknowns increases, the number of solution sets increases as well, and it requires great effort, if possible, to find the realistic solution.

FET serves as a faster version of Maas and Pope's classical ILDM method and their results have been shown to be very close to each other. The obvious question to ask is

whether or not they produce exactly identical results. Their results can be shown to be identical at least for Davis and Skodje's two-dimensional model discussed in section 4.1. As for the general case, either way hasn't been proven.

Bibliography

[1] G. E. Briggs and J. B. S. Haldane. A note on the kinetics of enzyme action. *Biochem. J.*, 19:339–339, 1925.

[2] Viatcheslav Bykov, Igor Goldfarb, Vladimir Gol'dshtein, and Ulrich Maas. On a modified version of ILDM approach: asymptotic analysis based on integral manifolds. *IMA J. Appl. Math.*, 2005.

[3] Nathaniel Chafee. The bifurcation of one or more closed orbits from an equilibrium point of an autonomous differential system. *J. Differential Equations*, 4:661–679, 1968.

[4] Michael J. Davis and Rex T. Skodje. Geometric investigation of low-dimensional manifolds in systems approaching equilibrium. *J. Chem. Phys.*, 111(3):859–874, 1999.

[5] Bard Ermentrout. *Simulating, Analyzing, and Animating Dynamical Systems.* Society for Industrial and Applied Mathematics, 2002.

[6] N. Fenichel. Geometric singular perturbation theory for ordinary differential equations. *J. Differ. Equ.*, 31:53–98, 1979.

[7] Simon J. Fraser. The steady state and equilibrium approximations: A geometrical picture. *J. Chem. Phys.*, 88:4732–4738, 1988.

[8] Alexander N. Gorban and Iliya V. Karlin. Method of invariant manifold for chemical kinetics. *Chem. Eng. Sci.*, 58:4751–4768, 2003.

[9] Alexander N. Gorban, Iliya V. Karlin, and Andrei Yu. Zinovyev. Constructive methods of invariant manifolds for kinetic problems. *Phys. Rep.*, 396:197–403, 2004.

[10] M. Hadjinicolaou and D. M. Goussis. Asymptotic solutions of stiff PDEs with the CSP method: the reaction diffusion equation. *SIAM J. Sci. Comput.*, 20:781–910, 1999.

[11] Jack K. Hale. *Ordinary Differential Equations.* Wiley-Interscience, New York, 1969.

[12] F. G. Heineken, H. M. Tsuchiya, and E. Aris. On the mathematical status of the pseudo-steady state hypothesis of biochemical kinetics. *Mathematical Biosciences*, 1:95–113, 1967.

[13] Hans G. Kaper and Tasso J. Kaper. Asymptotic analysis of two reduction methods for systems of chemical reactions. *Physica D*, 165:66–93, 2002.

[14] S. H. Lam. Using CSP to understand complex chemical kinetics. *Combust. Sci. Technol.*, 89:375–404, 1993.

[15] S. H. Lam and D. M. Goussis. Understanding complex chemical kinetics with computational singular perturbation. *Proc. Combust. Inst.*, 22:931–941, 1988.

[16] S. H. Lam and D. M. Goussis. The CSP method for simplifying kinetics. *Int. J. Chem. Kinet.*, 26:461–486, 1994.

[17] D. Lebiedz. Computing minimal entropy production trajectories: An approach to model reduction in chemical kinetics. *J. Chem. Phys.*, 120(15):6890–6897, 2004.

[18] F. A. Lindemann. *Trans. Faraday Soc.*, 17:598, 1922.

[19] U. Maas and S. B. Pope. Simplifying chemical kinetics: Intrinsic low-dimensional manifolds in composition space. *Combust. Flame*, 88:370–376, 1992.

[20] Leonor Michaelis and Maud Menten. Die kinetik der invertinwirkung. *Biochem. Z.*, 49:333–369, 1913.

[21] Isaac Newton. *De analysi per aequationes numero terminorum infinitas.* 1669.

[22] An Hoang Nguyen and Simon J. Fraser. Geometrical picture of reaction in enzyme kinetics. *J. Chem. Phys.*, 91:186–193, 1989.

[23] Joseph Raphson. *Analysis Aequationum Universalis.* London, 1690.

[24] Zhuyin Ren and Stephen B. Pope. Species reconstruction using pre-image curves. *Proc. Combust. Inst.*, 30:1293–1300, 2005.

[25] Marc R. Roussel. Forced-convergence iterative schemes for the approximation of invariant manifolds. *J. Math. Chem.*, 21:385–393, 1997.

[26] Marc R. Roussel. Invariant manifold methods for metabolic model reduction. *Chaos*, 11:196–206, 2001.

[27] Marc R. Roussel and Simon J. Fraser. Accurate steady-state approximation: implications for kinetics experiments and mechanism. *J. Phys. Chem.*, 95(22):8762–8770, 1991.

[28] Marc R. Roussel and Simon J. Fraser. On the geometry of transient relaxation. *J. Chem. Phys.*, 94(11):7106–7113, 1991.

[29] Rex T. Skodje and Michael J. Davis. Geometrical simplification of complex kinetic systems. *J. Phys. Chem. A*, 105:10356–10365, 2001.

[30] Steven H. Strogatz. *Nonlinear Dynamics and Chaos.* Addison-Wesley, 1994.

[31] C. A. Wurtz. Sur la papaïne: contribution à l'histoire des ferments solubles. *Compt. Rend.*, 91:787–791, 1880.